

Shelf-Basin Exchange in the Laptev Sea in the Warming Climate: a model study

Journal:	<i>Geophysical & Astrophysical Fluid Dynamics</i>
Manuscript ID:	GGAF-2014-0012.R1
Manuscript Type:	The dynamics of shelf seas Special Issue
Date Submitted by the Author:	n/a
Complete List of Authors:	Ivanov, Vladimir; Arctic and Antarctic Research Institute, Maslov, Pavel; OOO "Eco-Express-Service", Aksenov, Yevgeny; National Oceanography Center, Coward, Andrew; National Oceanography Center,
Keywords:	shelf-basin exchange, dense water cascading, Arctic ocean, sea ice , climate change

SCHOLARONE™
Manuscripts

1
2
3 1 **Shelf-Basin Exchange in the Laptev Sea in the Warming Climate: a model study**
4
5 2
6

7
8 3 **Vladimir Ivanov**¹: vladimir.ivanov@aari.ru, vivanov@iarc.uaf.edu
9

10 4 Arctic and Antarctic Research Institute, St.Petersburg, Russia
11

12 5 International Arctic Research Center, University of Alaska, Fairbanks, USA
13
14 6

15
16
17 7 **Pavel Maslov**: maasss@rambler.ru
18

19 8 OOO “Eco-Express-Service”, St. Petersburg, Russia
20
21 9

22
23
24 10 **Yevgeny Aksenov**: yka@noc.ac.uk
25

26 11 National Oceanography Centre, Southampton, UK
27
28 12

29
30
31 13 **Andrew Coward**: acc@noc.ac.uk
32

33 14 National Oceanography Centre, Southampton, UK
34
35 15
36
37 16
38
39
40

41 17 **Key words:** shelf-basin exchange, dense water cascading, Arctic Ocean, sea ice, climate change
42
43 18
44
45
46
47
48
49
50
51
52
53
54
55
56
57
58
59
60

¹ Corresponding author

Abstract. GCM-based forecast simulations predict continuously increasing seasonality of the sea ice cover and an almost ice-free, summer-time, Arctic Ocean within several decades from the present. In this study we use a primitive equation ocean model: NEMO, coupled with the sea ice model LIM2 to test the hypothesis that under such increased range in seasonal ice cover the intensity of shelf-basin water exchange will significantly increase. We use the simulated results for the Laptev Sea from a global model run 1958-2007 and compare results for two years with anomalously high/low summer sea ice extent: 1986-1987 and 2006-2007. The shelf-basin fluxes of volume, heat and salt during specific seasons are evaluated and attributed to plausible driving processes, with particular attention to dense water cascading. Analyses of the model temperature distribution at the depth of the intermediate maximum, associated with Atlantic Water, have demonstrated marked increase of the amount of the local origin cold water in late winter 2007 in the region, where dense water typically appears as a result of its formation on the shelf and subsequent downslope leakage. Calculation of the shelf-basin exchange during March-May in both years confirmed a substantial increase of fluxes in ‘ice-free’ 2007 compared to the ‘icy’ 1987, on the average by 2 times. According to several past model studies, dense water production on Arctic shelves in winter driven by ice freezing and salt ejection is not likely to cease in a warmer climate, but rather the opposite. There is also observational evidence that cascading in the seasonally ice covered seas (e.g. the Barents Sea) is much more efficient than it is in the permanently ice covered Arctic Ocean, which supports the presented model results.

1. Introduction

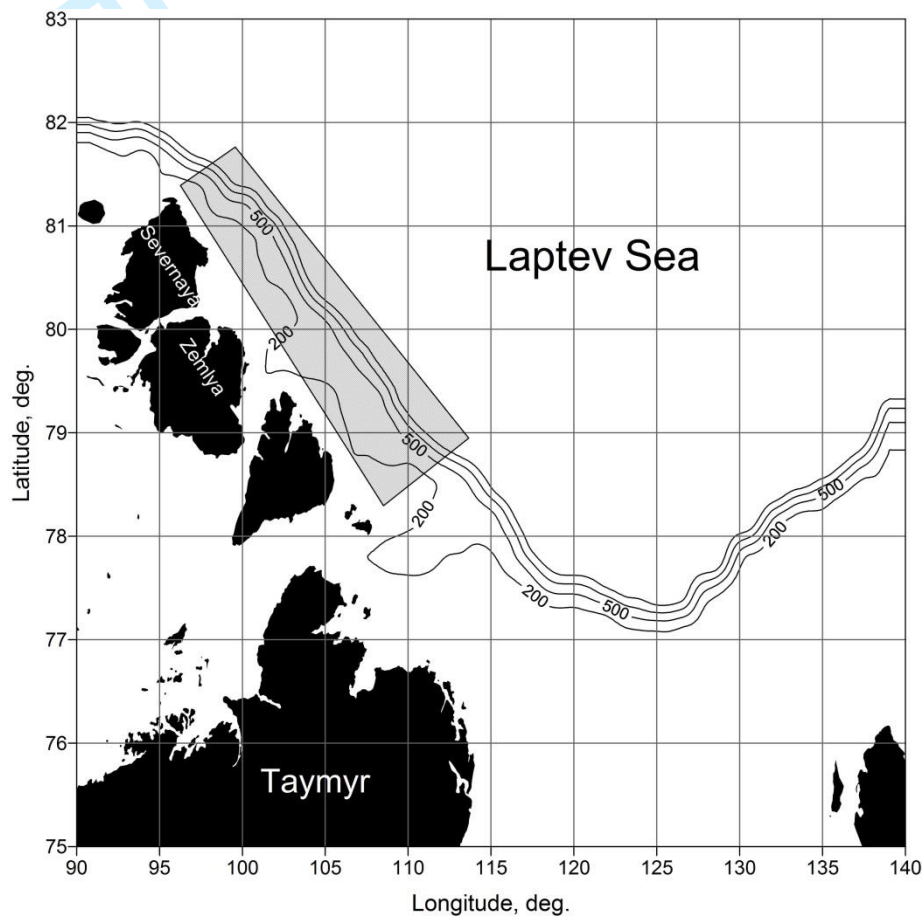
This study was motivated by substantial reduction of the summer sea ice in the Arctic Ocean in 1990-2010s, which accelerated after the “instant” decline of the ice-covered area in September 2007 by about 40% of the previous year seasonal minimum. In contrast with the summer ice extent, the winter one has not radically changed over these years. This seasonal dissimilarity eventually led to dominance of the first-year ice over the multiyear ice. Between 2004 and 2008 the

1
2
3 46 area of the first-year ice exceeded the area of the multiyear ice by about a factor of two (Kwok *et al.*
4
5 47 2009). GCM-based simulations predict continuously increasing seasonality of the sea ice cover and
6
7 48 almost ice-free Arctic Ocean in summer within several decades from the present. (CMIP5,
8
9
10 49 <http://pcmdi3.llnl.gov/esgcat>).

11
12 50 What consequences for the other components of the Arctic environment could we expect if
13
14 51 such scenario becomes reality? A retreating summer ice edge increases the size of the marginal ice
15
16
17 52 zones (MIZ) – the transient area between the open water and ice-covered ocean. Rapid changes in
18
19 53 the state of the ocean surface over the limited distance mean high horizontal gradients of properties
20
21 54 in oceanic and atmospheric boundary layers below and above the MIZ. High gradients trigger
22
23
24 55 strong motions in both strata, providing favorable prerequisite conditions for intensive horizontal
25
26 56 and vertical exchange of properties. In a general sense, decreasing ice cover is shifting the energy
27
28 57 balance at the sea-air interface to a higher level, which is characterized by intensified fluxes of
29
30
31 58 momentum, heat and moisture. In several past studies it has been shown that the retreat of the
32
33 59 summer ice edge in the Arctic Ocean also enhances horizontal and vertical exchange of water
34
35
36 60 across the shelf-break.

37
38 61 The efficiency of shelf-basin exchange in the areas neighboring the MIZ is strongly
39
40 62 controlled by the location of the ice edge relative to the bottom topography. In summer season
41
42
43 63 retreat of the ice edge seaward of the shelf-break favors wind-induced upwelling to deliver salty,
44
45 64 nutrient-rich water from the deep on shelf (Carmack and Chapman 2003). Continuous retreat of the
46
47
48 65 ice cover exposes waters off the shelf-break for longer periods of time, increases the intensity of
49
50 66 upwelling, efficiency of mixing and shelf-basin exchange (Pickart et al 2009, Rainville et al, 2011).
51
52 67 In winter season, when the Arctic Ocean is almost totally covered by ice, pockets of active shelf-
53
54 68 basin water exchange are associated with latent-heat polynyas – extended openings in the ice cover,
55
56
57 69 which separate fast and pack ice (Maqueda et al. 2004). Dense water, forming inside polynyas as a
58
59 70 result of freezing and brine ejection, leaks down the continental slope in shape of bottom boundary
60
71
72 71 current (cascading). Shelf-slope cascading invokes compensatory ascending flow of the deep water
72
73 72 onto the shelf, providing efficient means of shelf-basin water exchange (Kampf 2005, Ivanov and

73 Golovin 2007). Similar to upwelling, polynyas are generated by the favorable wind which breaks up
 74 the fast ice and moves ice floes offshore (Pease 1987). Later onset of freezing, due to progressive
 75 degradation of the summer ice cover, predisposes thinner ice during the next winter (Stroeve et al.
 76 2011). Thinner ice is more mobile and fragile, thus being stronger affected by the wind stress.
 77 Thence, we may anticipate that in the warming climate shrinking summer ice cover should facilitate
 78 shelf-basin water exchange throughout the entire year.



79
 80 Figure1. The study area. Smoothed bottom topography of the shelf-slope is shown by solid lines.
 81 Polygon marks the region, where flux calculations were performed.

82
 83 In this study we use hindcast results from a primitive equation ocean model NEMO
 84 (Madec et al. 1998), coupled with the sea ice model LIM2 (Fichefet and Maqueda 1997) to test this
 85 hypothesis in the Laptev Sea (Figure 1). The Laptev Sea plays very specific role in shaping the
 86 Arctic Ocean climate conditions. The major Arctic surface current - the Transpolar Drift,
 87 predominantly originates in the northern Laptev Sea and transports sea ice towards Fram Strait
 88 (Wiese 1948, Nikiforov and Shpaikher 1980, Krumpfen et al. 2013). Intensity of the Transpolar Drift

is controlled by the prevailing atmospheric forcing - cyclonic/anticyclonic (Proshutinsky and Johnson 1997). The type of atmospheric circulation also preconditions local hydrography by changing the pathways of riverine waters (Dmitrenko et al. 2010a, Morison et al. 2012), and facilitating/impeding shelf-slope exchange due to cascading/upwelling (Rudels et al. 2000, Dmitrenko et al. 2010b). The Laptev Sea shelf is a prominent dense water formation site (Aagaard et al. 1981, Martin and Cavalieri 1989, Dethleff 2010). Cold dense water, which forms in winter polynyas on the north-western shelf, cascades into adjacent deep basin, modifying AW (Ivanov and Golovin 2007), which circulates cyclonically around the major Arctic basins (Rudels et al. 1994).

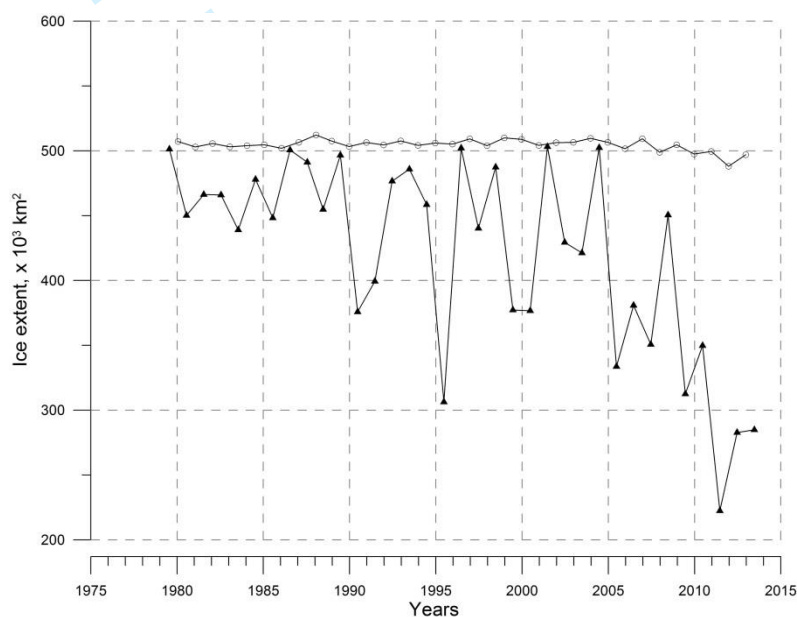


Figure 2. Time series of ice extent (15% concentration) according to satellite data: open circles denote winter season (Dec – May), triangles denote summer season (Jun – Nov) (Cavalieri 1996, <http://nsidc.org/data/nsidc-0051.html>).

In 1990-2010s sea ice conditions in the Laptev Sea have undergone similar changes as those on the pan-Arctic scale. Seasonality of the ice cover substantially increased after 2005 (Figure 2), while the mean ice thickness had diminished (Frolov et al. 2009). This observed rapid transition provides an opportunity to test theoretical hypotheses on the effect of the sea ice state on shelf-slope exchange. The goal of this study is to quantify the range of possible effects produced by increasing seasonality of the sea ice cover on shelf-basin exchange in the Laptev Sea. To achieve this goal, we used results of the global NEMO-LIM2 model run 1958-2007. We post-processed and analyzed the

1
2
3 109 yearly model output with respect to the Laptev Sea for two years with high/low summer ice extent:
4
5 110 1986-1987 and 2006-2007 (see Figure 2). The major target of the analysis was the evaluation of
6
7 111 shelf-basin fluxes of volume, heat and salt during specific seasons and their attribution to plausible
8
9
10 112 driving processes, with particular attention to dense water cascading.
11

12 113 The paper consists of 5 sections. In the second section we briefly describe the
13
14 114 configuration of the global NEMO model used for this study. In Section 3 we present model results
15
16 115 with respect to the Laptev Sea, and compare model output with available observations and satellite
17
18
19 116 data. Calculation of fluxes and their comparative analysis for two selected years is carried out in
20
21
22 117 Section 4. Discussion of obtained results and general conclusions finalize the paper.
23
24 118

26 119 **2. Methods**

28 29 120 **2.1 Global NEMO-LIM2 configuration**

30
31 121 The Nucleus for European Modelling of the Ocean (NEMO) is a state-of-the-art modeling
32
33 122 framework for oceanographic research, operational oceanography seasonal forecast, and climate
34
35 123 studies (<http://www.nemo-ocean.eu/>). The NEMO ocean model is a primitive equation model
36
37
38 124 OPA9 (Madec et al. 1998) adapted to regional and global ocean circulation experiments. It is
39
40 125 designed to be a flexible tool for studying the ocean and its interactions with other components of
41
42
43 126 the earth climate system (in particular sea-ice) over a wide range of space and time scales.
44
45 127 Prognostic variables are the three-dimensional velocity field, a linear or nonlinear sea surface
46
47
48 128 height, temperature, and salinity. In the horizontal direction, the model uses a curvilinear orthogonal
49
50 129 grid and in the vertical direction, a full- or partial-step z-coordinate, or s-coordinate, or a mixture of
51
52 130 the two. For the present study the model is configured on a common tri-polar Arakawa C-grid with
53
54
55 131 the poles placed at the geographical South Pole, in Siberia and in the Canadian tundra. The grid has
56
57 132 a horizontal resolution of 6-12 km in the Arctic Ocean admitting larger ocean eddies. There are 75
58
59 133 vertical levels (1-41 m thick in the upper 400 m, increasing to 204 m thick at 6000 m). For these
60
134 simulations (1958–2007), the model was driven by the Common Ocean-Ice Reference Experiments
135 (CORE2) dataset. The ocean model is coupled to the Louvain-la-Neuve sea ice model LIM2

1
2
3 136 (Fichefet and Maqueda 1997), updated for the use in the high-resolution configurations (Johnson et
4
5 137 al. 2012). NEMO simulations have been thoroughly analysed and evaluated against the available
6
7 138 observational data in the Arctic Ocean Intercomparison Project (AOMIP, Proshutinsky et al. 2011)
8
9
10 139 and show good agreement with observed fields in the Arctic and subarctic seas, such as sea ice
11
12 140 concentration and thickness, mixed layer depth and with the observed oceanic fluxes through the
13
14 141 key straits connecting the Arctic Ocean to the World ocean (Lique et al. 2009, Jahn et al. 2012,
15
16
17 142 Johnson et al. 2012).

21 144 *2.2. Calculation of fluxes*

22
23
24 145 Generally, the significance of a specific physical processes to the maintenance of the given
25
26 146 climate state of the system (ocean, atmosphere etc.) is assessed by some measurable parameters,
27
28
29 147 which may characterize the overall (bulk) intensity of the considered process. The bulk components
30
31 148 of the climatic structure of the ocean are water masses – large bodies of water with nearly similar
32
33 149 temperature and salinity characteristics (Encyclopaedia Britannica 2014). Changes of
34
35
36 150 temperature/salinity within water masses are caused by horizontal and vertical fluxes of heat/salt
37
38 151 across their boundaries. Hence, the magnitude of heat/salt fluxes between water masses, associated
39
40
41 152 with the studied process may serve as a measure of the efficiency of this process in changing the
42
43 153 given state of the ocean. In this study we were interested in changes of shelf-basin water exchange
44
45 154 in the Laptev Sea, which may be quantitatively characterized by changes in corresponding heat/salt
46
47
48 155 fluxes.

49
50 156 At the post-processing stage model results were used for calculating volume/heat/salt
51
52 157 fluxes (F_k) according to the algorithm introduced in (Ivanov and Golovin 2007):
53
54
55 158

$$57$$

$$58 159 F_k(x_1, x_2, z_1, z_2, t) = \frac{1}{(x_2 - x_1)(z_2 - z_1)} \int_{x_1}^{x_2} dx \int_{z_1}^{z_2} \Delta K \cdot v_n dz \quad (*)$$

$$59$$

$$60$$

160

1
2
3 161 where $\mathbf{K}(l, \rho c_p T, \rho S)$ is ‘vector’ with components, describing water volume, heat, and salt content;
4
5 162 ΔK is the horizontal contrast between shelf and the deep water; v_n is the velocity component normal
6
7 163 to bottom topography and directed offshore; dx is the unit distance along the topography contour
8
9
10 164 $z=H(\lambda, \theta)$ between the selected lateral boundaries x_1 and x_2 ; dz is the unit distance between the
11
12 165 selected lower and upper boundaries z_1 and z_2 . Formula (*) gives specific fluxes of water volume,
13
14 166 heat, and salt through the square with bounds x_1, x_2, z_1 and z_2 in conventional system units: m/s,
15
16
17 167 W/m^2 and g/sec/m^2 respectively.
18

19 168 The exact location of the interface between shelf and deep water masses in the Laptev Sea
20
21
22 169 is variable in time and unknown *a priori*. In this study we used the approach, used in (Ivanov and
23
24 170 Golovin 2007), and took bottom topography contours (z_1) as foundations of 2-dimensional vertical
25
26 171 surfaces to calculate the flux through. In flux calculations, z_1 continuously increased from the depth
27
28
29 172 of the shelf to the depth of the mid-slope. The upper integration limit (z_2) was permanently equal to
30
31 173 zero, implying the ocean surface. Lateral bounds (x_1 and x_2) were taken in accordance with existent
32
33 174 knowledge on the Laptev Sea hydrography. We considered specific region (polygon in Figure 1),
34
35
36 175 which is prominent for cascading events (Ivanov et al. 2004, Bareiss and Goergen 2005).
37
38 176
39

40 177 **3. Modelled sea ice, thermohaline properties and currents**

41
42
43 178 A detailed analysis of the NEMO model results with respect to the Arctic Ocean
44
45 179 thermohaline structure, ocean dynamics, exchanges through the Arctic straits and sea ice and their
46
47
48 180 temporal variability can be found in (Jahn et al. 2012, Johnson et al 2012, Lique and Steele 2012,
49
50 181 Jackson et al. 2014). Brief discussion of differences in the pan-Arctic circulation in September 1987
51
52 182 and 2007 is provided in the supplement file. In this section we focus on the results of simulation for
53
54
55 183 the Laptev Sea around annual (September – September) for two studied years with substantially
56
57 184 different ice conditions, shown in Figure 3 and 4. As follows from these figures, modelled monthly
58
59 185 mean ice extent and ice concentration in the Laptev Sea reasonably coincides with the actual one,
60
186 reconstructed from the DMSP (Defence Ministry Satellite Program) SSMR and SSM/I satellite data
187 (Cavalieri 1996, <http://nsidc.org/data/nsidc-0051.html>).

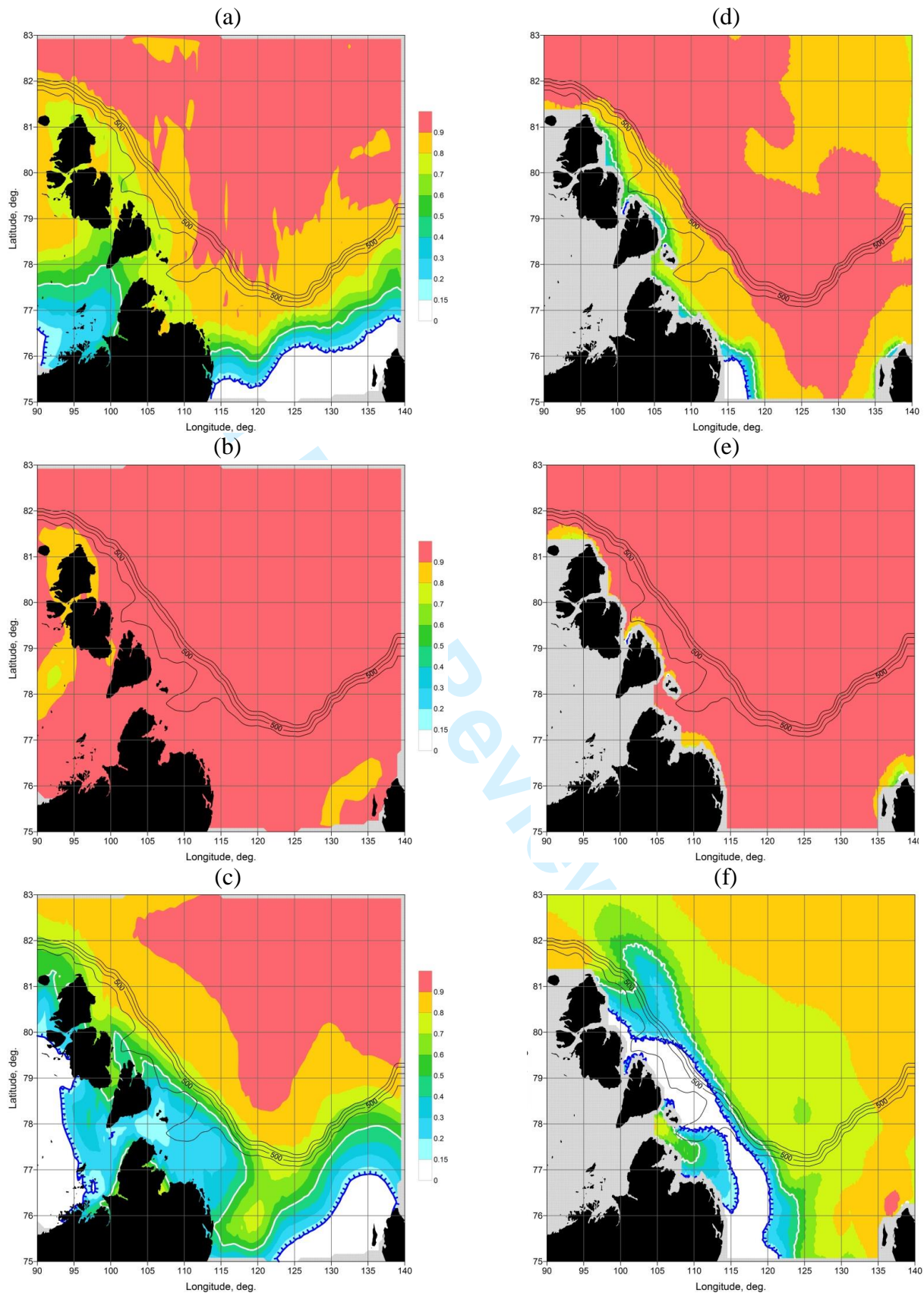


Figure 3. Mean monthly ice concentration in 1986-87: September-1986, April-1987, September-1987 according to satellite data (a, b, c) and model calculations (d, e, f) respectively.

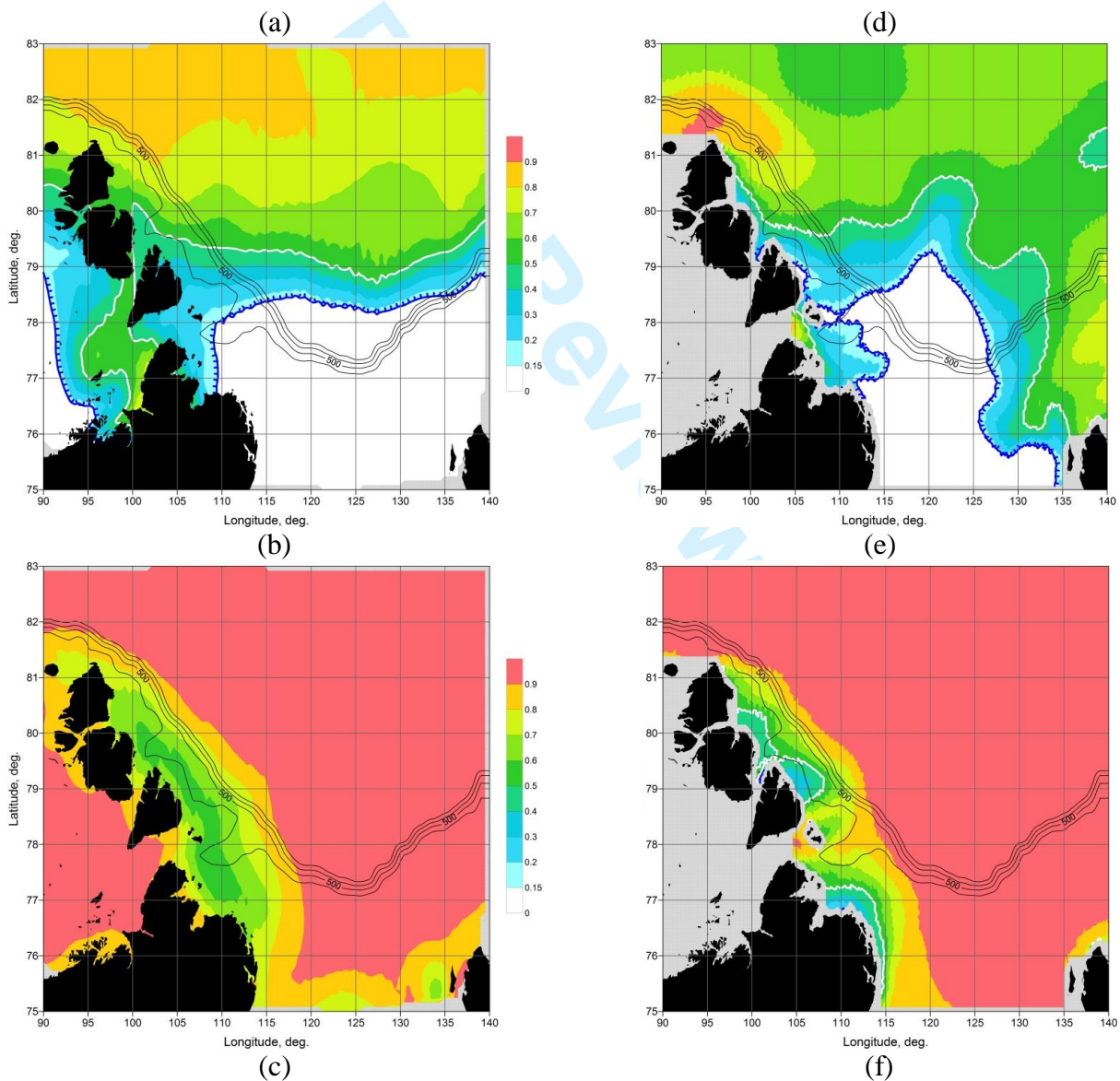
188

Although the exact patterns differ in specific regions, the average deviation of the model

189

data from the actual total ice concentrations within the studied area over 1986-87 and 2006-2007

1
2
3 190 does not exceed 14%. This coincidence is generally better in 1986 -1987 and in winter time. The
4
5 191 largest deviation of the model from the actual ice concentration is observed in September 2007,
6
7 192 when model data underestimate actual ice retreat (Figure 4-c, f). It is important to draw attention to
8
9
10 193 very close similarity between locations of western Severnaya Zemlya polynya in April 2007 in the
11
12 194 model and in the satellite data (Figure 4-b, e). The most intensive cascading in this region typically
13
14 195 occurs in March-April, when the water column on shelf is pre-conditioned by thermohaline
15
16 196 convection through the cold season (Ivanov et al. 2004), and additional input of salt, resulting from
17
18 197 ice freezing inside polynya triggers cascading (Ivanov and Golovin 2007).



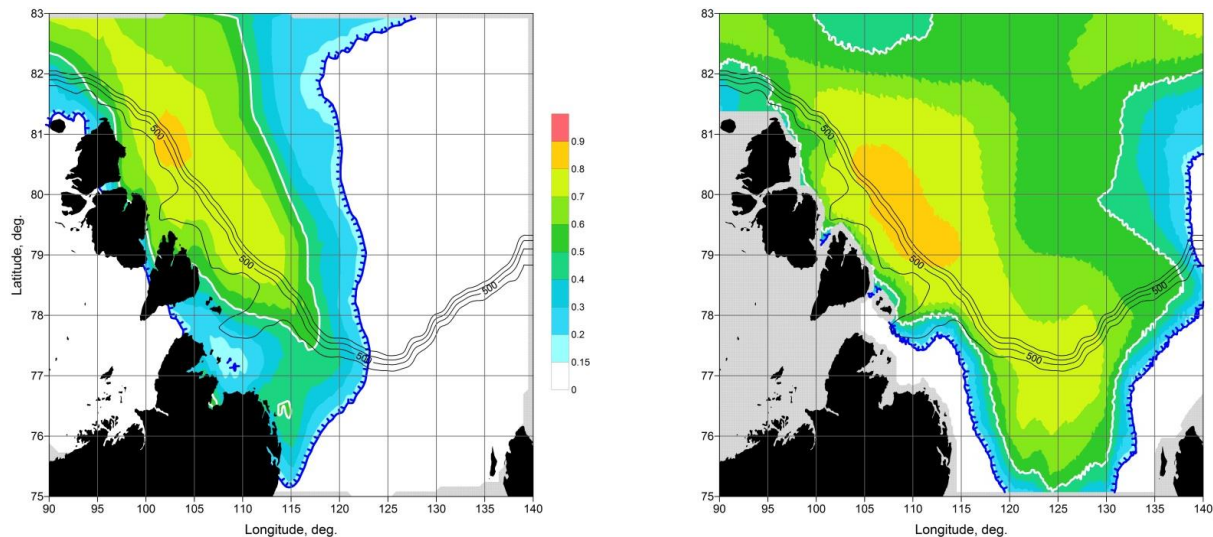


Figure 4. Mean monthly ice concentration in 2006-07: September-2006, April-2007, September-2007 according to satellite data (a, b, c) and model calculations (d, e, f) respectively.

Thermohaline conditions in the intermediate water layers of the Laptev Sea (from the depth of the outer shelf, about 100-120 m to 1000-1500 m over the continental slope) is controlled by three branches of Atlantic Water, Fram Strait Branch (FAW), Barents Sea Branch (BAW), shelf branch (SAW) and their interactions (Rudels 2013, Ivanov and Aksenov 2013). The existence of the SAW was predicted in the recent model study by (Aksenov et al. 2011) and is so far confirmed by indirect observational evidence. The major heat and salt influx into the Laptev Sea is provided by the FAW. The warm core of the FAW in the studied area is embedded at 230 – 270 m depth (EWG 1997, 1998). Therefore, we have focused on the 250 m depth to depict characteristic features of thermohaline and dynamical spatial structure, replicated by the model. As follows from Figure 5, general pattern of temperature and currents has not radically changed over the 20 years under review. FAW enters the studied area in the north-western corner and moves generally to the east, gradually losing heat due to horizontal and vertical mixing (Rudels 1994, Ivanov and Aksenov 2013). The strongest flow occurs in the narrow boundary current, which, according to the model retrospective, contains the SAW, originated in the north-eastern Barents Sea (Aksenov et al. 2011). FAW core is not associated with high current speed. There are several differences between Figure 5 (a) and (b). The most noticeable features are in the intensity of temperature maximum (higher) and temperature minimum (lower) in September 2007. Positive temperature shift in 2007 from 1986 is

likely an indication of continuous AW warming in the Arctic Ocean after 1990 (Polyalov et al. 2005), captured by the model. Our explanation of the lower temperature minimum in September 2007 is based on the hypothesis that a decisive contribution is made by dense water forming and cascading, to the depth of FAW warm core in late winter 2007.

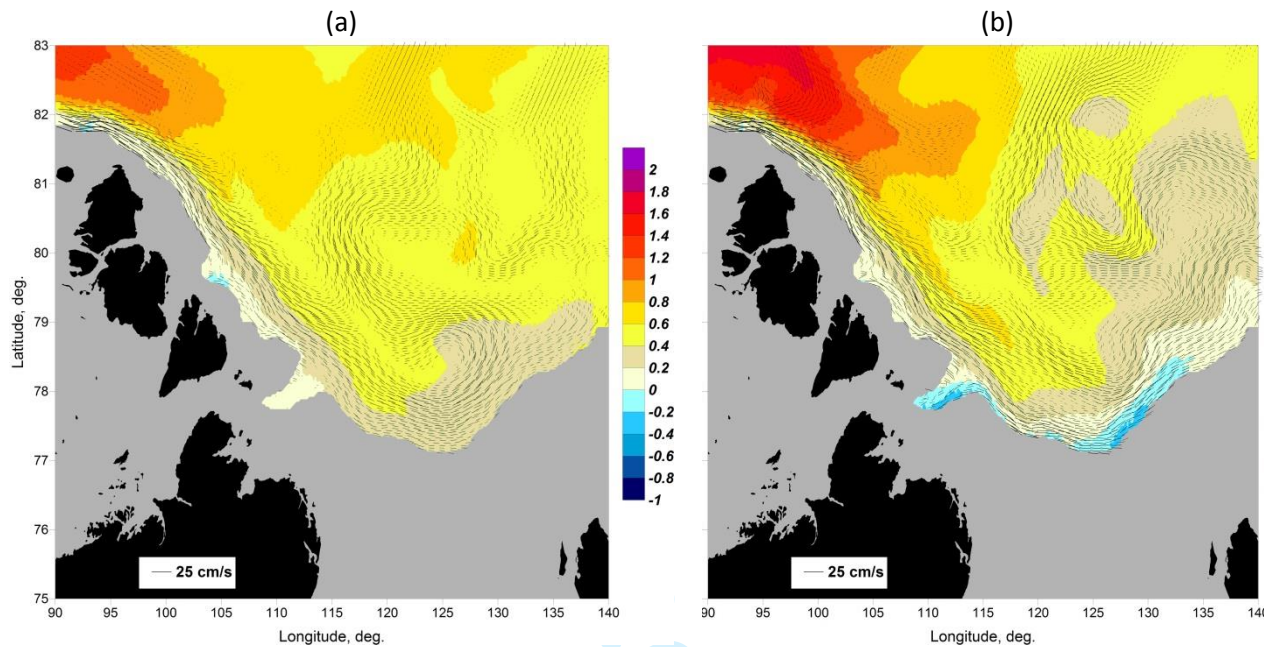
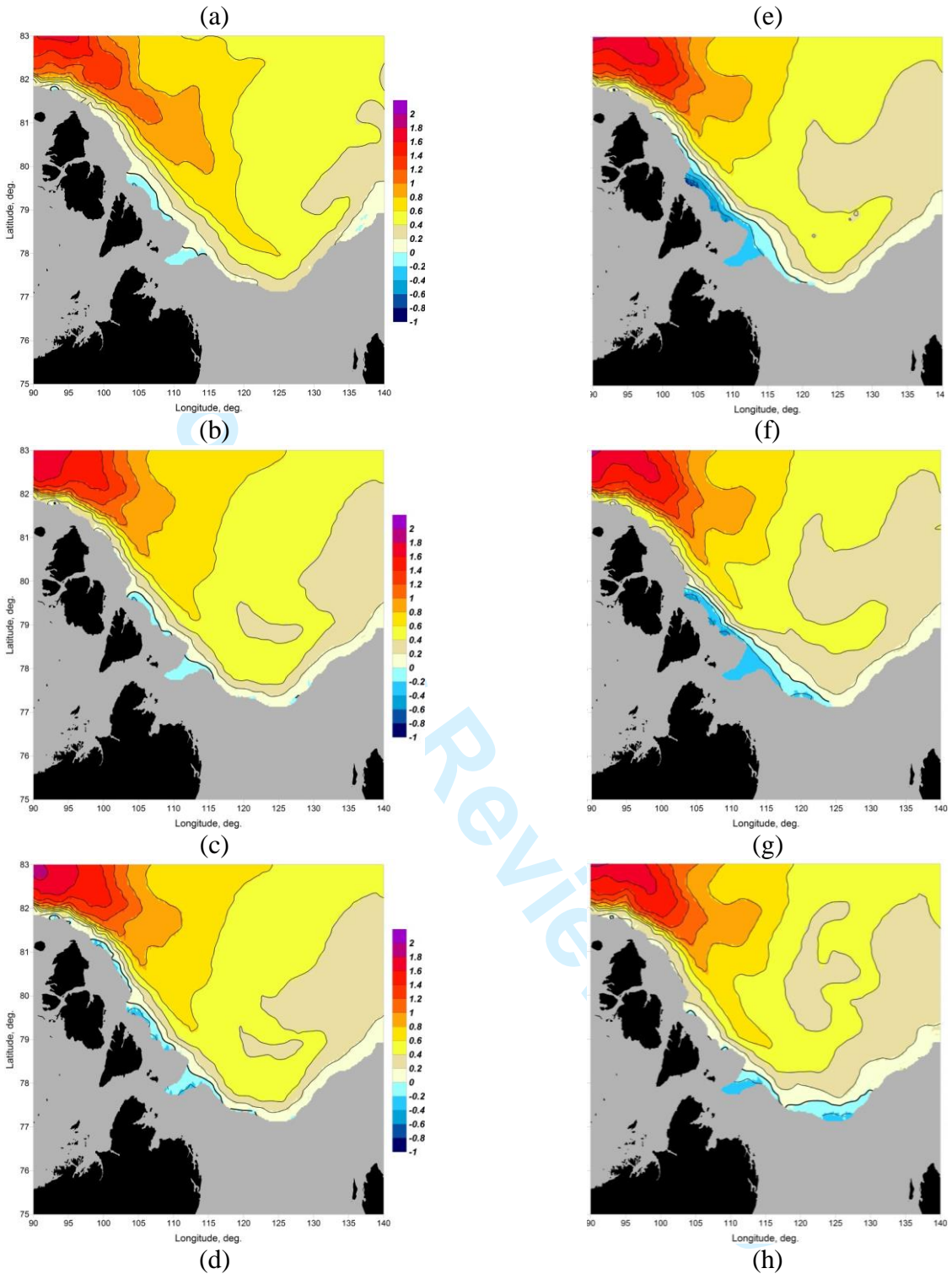


Figure 5. Model distribution of monthly mean temperature, °C, and current speed, cm/s at 250 m depth in September, 1986 (a) and 2007 (b).

Sequential temperature maps at 250 m from September 2006 to September 2007 are presented in Figure 6. There is no noticeable difference in location and intensity of the cold water zones from September 2006 (a) through February 2007 (b). An elongated spot with the temperature slightly below zero is sitting at the slope, in and between two relatively deep tranches, cutting the continental slope of the north-western Laptev Sea at about 78°E and 80°E. This distribution starts changing in March 2007 (c), when the zone with negative temperature extends intermittently north-westwards along the slope, while the minimum temperature goes down. In April 2007 (d) local pockets of substantially colder water (< -0.7) appear within the northern trench. This cold water may not be advected by the boundary current, because there is no signs of water that cold upstream. From May (e) through July (f) the cold water moves south-eastwards along the slope gradually filling the southern trench and decreasing the temperature there.

1
2
3
4
5
6
7
8
9
10
11
12
13
14
15
16
17
18
19
20
21
22
23
24
25
26
27
28
29
30
31
32
33
34
35
36
37
38
39
40
41
42
43
44
45
46
47
48
49
50
51
52
53
54
55
56
57
58
59
60



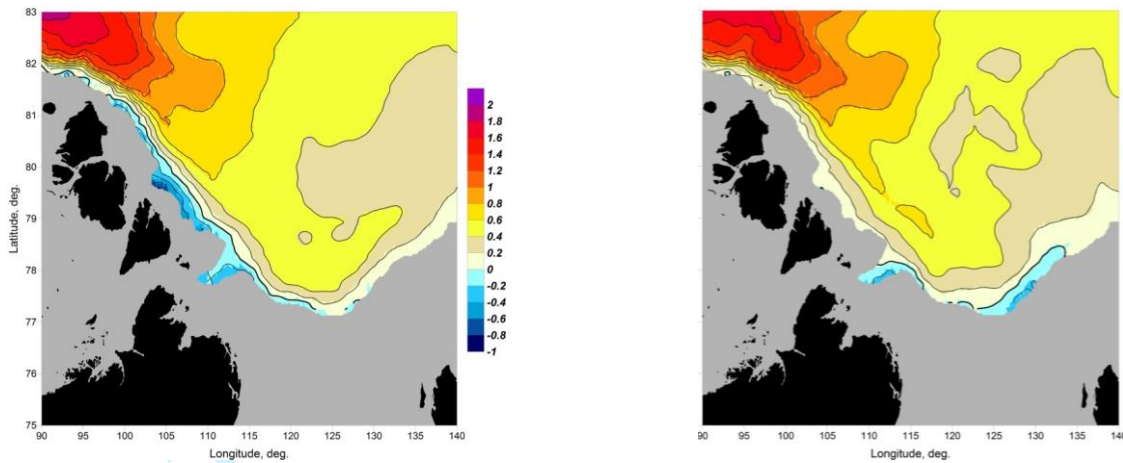


Figure 6. Model temperature distribution ($^{\circ}\text{C}$) at 250 m throughout 2006-07: (a) Sep-2006; (b) Feb-2007; (c) Mar-2007; (d) Apr-2007; (e) May-2007; (f) Jul-2007; (g) Aug-2007; (h) Sep-2007. Contours show smoothed temperature field.

In August (g) and September (h) 2007 the tongue of cold water circulates around the southernmost point of the Laptev Sea shelf and turns with the bathymetry to the north-east. It is important to note, that by September, 2007 there is no cold water in the region of its origin – the trench at 80°N .

The evolution of cold anomalies, replicated in the model, confirm our working hypothesis of the ‘shelf convection – cascading’ nature of this phenomenon. According to previous studies, the most suitable site in the Laptev Sea, where dense water, generated in the local polynya, is able to attain sufficient density to cascade as deep as the FAW core, is located on the shelf adjoining the trench at 80°N (Ivanov et al. 2004). Depending on the actual atmospheric forcing and parameters of the local polynya (size and frequency of opening through the winter), water with cascading potential may reach various water layers over the neighbouring continental slope (Ivanov and Watanabe 2013). According to modelling results, the most effective leaking of dense water downslope occurs through the trench, invoking compensatory deep water flow on shelf (Ivanov and Golovin 2007). The timing, which is required for dense water to reach the 250 m depth in the trench at 80°N is about 100 days, starting from the point, when shelf convection has totally homogenized the water column over the shallow (about 50 m depth) bank (Ivanov and Golovin 2007: Figure 10). Applying this timing to the current simulations suggests that to get first indications of new portion

of dense water in the trench in March, the shelf convection should mix the water column over the shallow bank by late November – early December. This is entirely feasible, taking into account

1

2

3

4

5

6

7

8

9

10

11

12

13

14

15

16

17

18

19

20

21

22

23

24

25

26

27

28

29

30

31

32

33

34

35

36

37

38

39

40

41

42

43

44

45

46

47

48

49

50

51

52

53

54

55

56

57

58

59

60

61

62

63

64

65

66

67

uncertainties in the polynya dynamics. Formation of dense water on the north-eastern Laptev Sea shelf in winter 2006-07, and down-slope cascading of this water is described in details in the supplement file.

Another result in favour of our concept follows from Figure 7, which shows the time series of maximum and minimum temperature at 250 m in 1986-87 and 2006-07. Two top lines are rather similar, indicating existence of seasonal cycle in the FAW, which is mostly transported from upstream by the boundary current (Ivanov et al. 2009; Dmitrenko et al. 2009). Time evolution of the 1986-87 temperature minimum also shows well-pronounced seasonal cycle. Although this curve is shifted in phase from the upper lines, there is no indication of any disturbances, associated with specific season. Time evolution of 2006-07 temperature minimum is very different. Instead of quasi-regular seasonal variation, there is rapid temperature drop, starting in March with culmination in May, and restoration in July to the numbers, close to those in the previous September.

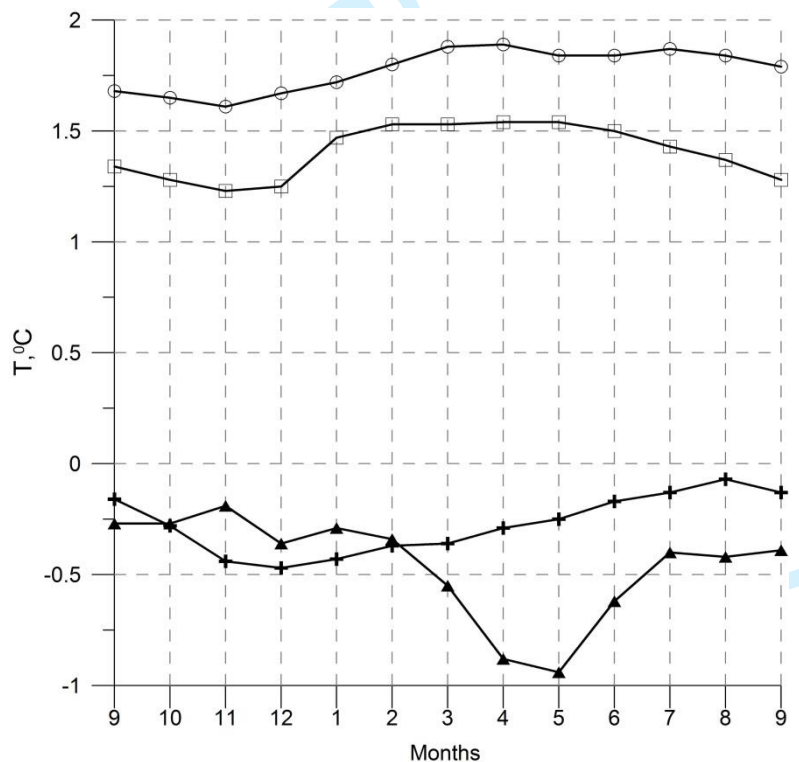


Figure 7. Time series of maximum and minimum temperature at 250 m depth in 1986-87 and 2006-07: T_{\max} in 1986-87 - open squares; T_{\max} in 2006-07 - open circles; T_{\min} in 1986-87 - crosses; T_{\min} in 2006-07 - triangles.

Evidence of intensive cascading development in the north-western Laptev Sea in April

2007 is provided by vertical temperature and salinity distribution across the continental slope.

Vertical sections along 80°N in April 1987 and 2007 are presented in Figure 8. The difference in the

pattern of thermohaline properties at the slope is very well distinguished in these plots. In April,

1987 relatively strong halocline (0.3 PSU) separates the water at the 100 m depth from the cold

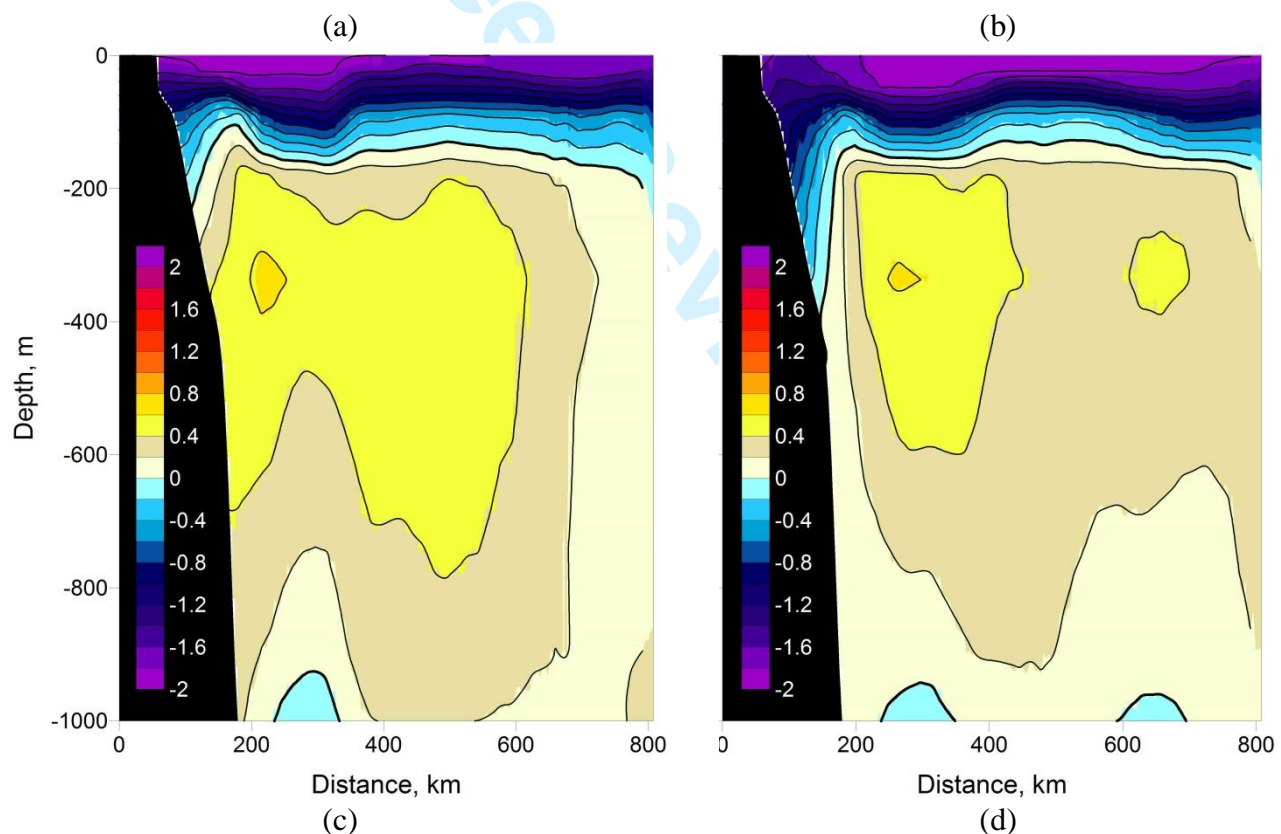
(near to freezing temperature) and fresher water at the surface (b). In April 2007, almost

homogeneous water layer with salinity around 34.55 PSU is reaching the depth of 350 m (Figure 8,

c), thus allowing deep penetration of the cold water from the surface (d). As a result, in April 1987,

warm Atlantic water (with temperature above zero) is bordering the slope at about 200 m depth,

while in 2007 this water is detached from the slope down to the depth of 400 m (Figure 8, b, d).



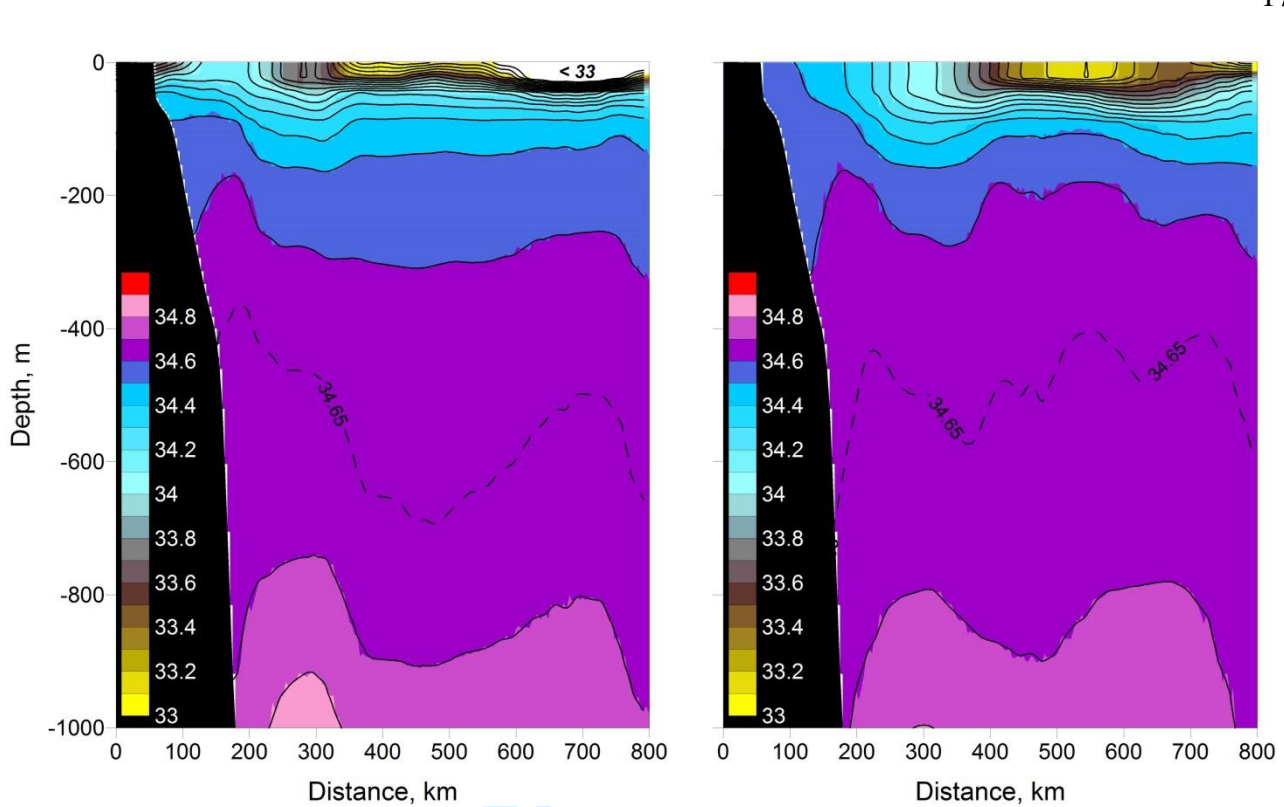


Figure 8. Temperature ($^{\circ}\text{C}$) and salinity (PSU) distribution at the vertical section along 80°N in April 1987 (a,c) and in April 2007 (b,d) respectively.

4. Shelf-basin fluxes

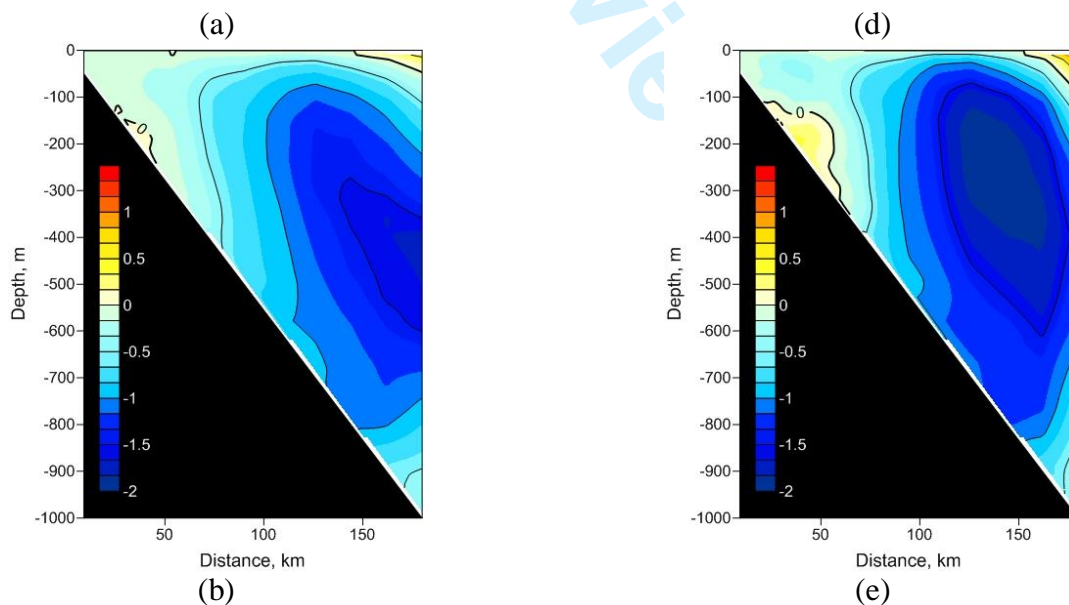
Change in the intensity of shelf-basin exchange between late winter – spring 1986-87 and 2006-07, depicted in the previous section, is quantified by cross-slope fluxes of volume, heat and salt, calculated in accordance with formula (*) for the region, marked by the polygon in Figure 1.

Vertical distribution in Figure 9 shows horizontally averaged specific fluxes per unit square, which is oriented perpendicular to the bottom topography gradient. Spatial step, used in calculations was taken equal to 50 m for the depth range 0-500 m, and 100 m, from 500 to 1000 m depth. Offshore direction is defined as the positive one.

Specific volume flux (m/s) in this case is equivalent to the cross-topography component of the flow speed. As follows from Figure 9 (a, d), the plane of the transect in both years is divided into two zones with opposite direction of cross-isobath flow. In the deeper part, which is roughly bounded by 350 m depth at the slope, the flow is directed onshore with maximum speed near the deep end of the transect. The largest difference between the two studied years is observed in the

1
2
3 293 shallow corner of the transect. In April, 1987 the zone of positive (offshore) flow is confined to
4
5 294 small region around 200 m depth at the slope (a), while in April 2007, there is much more extended
6
7 295 zone of the offshore flow, encompassing the segment of slope from 150 m to 300 m (d). The
8
9
10 296 maximum speed and especially the offshore one, is higher in 2007. There is an explicit circulation
11
12 297 cell in the zone between 0 and 70 km distance, with offshore motion near the bottom and onshore
13
14 298 motion above it. This circulation cell is an indication of cross-slope dynamics, typical for
15
16
17 299 ‘cascading-upwelling’ events (Ivanov and Golovin 2007).

18
19 300 There is a remarkable difference in heat flux between two compared years (see Figure 9-b,
20
21 301 e). In April 1987, the heat flux below 100 m is generally low and around zero. In April 2007, there
22
23 302 are three very well distinguished zones with opposite signs and high intensities of the heat flux. The
24
25 303 negative flux zone in the left corner completely coincides with the area of the strong offshore flow
26
27 304 (compare: Figure 9 d, e). Since the direction of the flow in this zone is positive, negative heat flux
28
29 305 means that colder water is transported offshore. As was shown in the previous section, this cold
30
31 306 water is apparently the shelf origin water, which is leaking downslope.



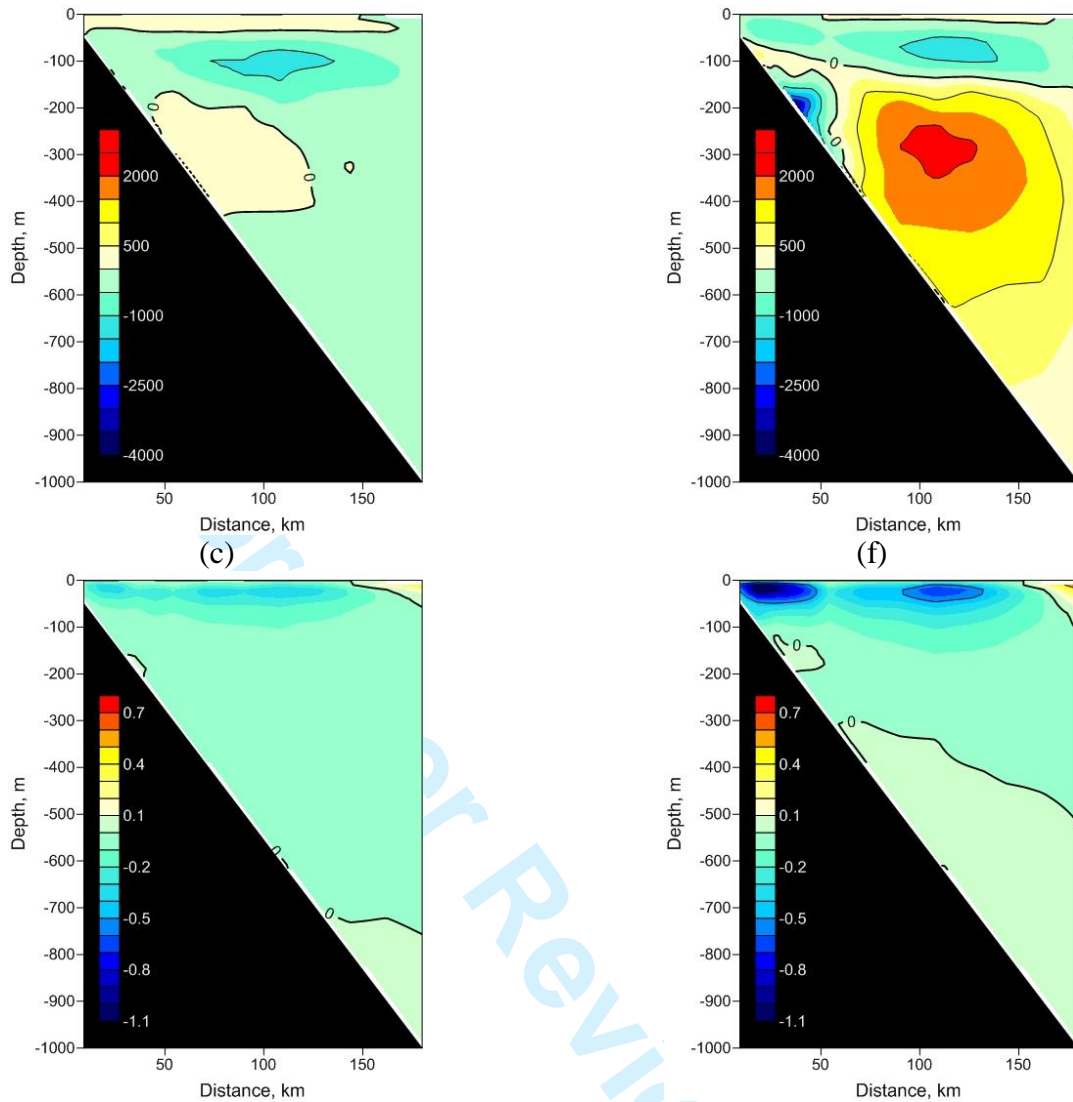


Figure 9. Vertical distribution of mean cross-slope speed of flow, m/s (a, d); specific heat flux, W/m^2 (b, e); salt flux, g/m/s (c, f) in March - May 1987 and 2007. Spatial averaging is done over depth contours with lateral bounds, shown in Figure 1.

Negative heat flux above 100 m reflects the onshore flow of warmer water from the deep basin. In the shallow part of the transect (0 -70 km distance) this heat flux is probably associated with compensatory upwelling, which accompanies cascading (Ivanov and Golovin 2007). The deep zone with positive heat flux probably reflects the heat exchange within FAW, which is characterised by stronger temperature irregularity in April, 2007, compared to April, 1987.

Salt flux associated with cascading in the Laptev Sea typically changes sign with increasing depth (Ivanov and Golovin, 2007). This happens because of salinity stratification, which makes the water, which sinks in the process of cascading, saltier than the ambient water while passing the halocline, and fresher when reaching the salty FAW core (see Figure 8-d). This is

1
2
3 317 reflected in Figure 9-f by the compact zone with positive salt flux around 200 m depth on the slope
4
5 318 and small negative flux further down the slope. High negative salt flux near the surface in both
6
7 319 years is associated with onshore motion of salty water from the basin, which is stronger in April
8
9
10 320 2007, because of compensatory upwelling.

11
12 321 Overall, the analysis of cross-slope fluxes of volume, heat and salt points out that in April
13
14 322 2007 the intensity of shelf-basin exchange was substantially higher, than in April 1987. This
15
16 323 difference was especially pronounced at the upper slope and was associated with more intensive
17
18 324 development of cascading. Quantitatively, mean fluxes in two compared cases (April, 1987 and
19
20 325 April, 2007) were: speed of the flow was 0.38 m/s and 0.44 m/s; specific heat flux was 71 W/m²
21
22 326 and 246 W/m²; specific salt flux was 0.018 g/m²/s and 0.034 g/m²/s correspondingly. The obtained
23
24 327 results and the limits of their applicability for the seasonally ice free Arctic Ocean are discussed in
25
26 328 the next section.

33 330 5. Discussion and conclusions

34
35 331 Accelerated reduction of the summer ice cover after 2007 led to the dominance of the first-
36
37 332 year ice in the Arctic Ocean. Overall result of this tendency (if sustained, as predicted in the recent
38
39 333 CMIP5 model simulations, cited in the Introduction, and in the IPCC report (2007)), will be
40
41 334 increased seasonal range of ice cover and thinner, more fragile sea ice in winter. In this model study
42
43 335 we examined, how such changes in the ice cover properties may affect the shelf-basin exchange due
44
45 336 to expected intensification of dense water formation on shelf and cascading of this dense water to
46
47 337 the adjacent deep basin. We targeted the north-western shelf-slope region in the Laptev Sea,
48
49 338 because of its well-known high potential to produce sufficiently dense water in the past. The
50
51 339 monthly mean output of the NEMO-LIM2 model experiment was analysed for two years with very
52
53 340 different ice conditions: 'icy' 1986-87 and 'ice-free' 2006-07. Analysis of temperature distribution
54
55 341 at the depth of the FAW maximum in the Laptev Sea (250 m) have demonstrated visible increase of
56
57 342 the amount of the local origin cold water in late winter 2007 in the region, where this dense water
58
59 343 typically appears as a result of its formation on shelf and downslope leaking. Time evolution of the

1
2
3 344 minimum temperature at the 250 m depth revealed a radically different shape of the temperature
4
5 345 minimum curve in 2007 compared to that in 1986-87. The later one exhibits quasi-regular seasonal
6
7 346 cycle, similar to the time evolution of maximum temperature in both studied years. In 2007 the
8
9
10 347 seasonal cycle is disturbed by a strong decrease of minimum temperature in March-June, which
11
12 348 coincides with the timing, when dense water cascading is at its maximum (Shapiro et al. 2003).
13
14 349 Quantitative analysis of the shelf-basin exchange during March-May in both years on the basis of
15
16
17 350 calculated volume, heat and salt fluxes confirmed a substantial increase of fluxes in 'ice-free' 2007
18
19 351 compared to the 'icy' 1987, on the average by 2 times.

20
21
22 352 According to several past model studies, dense water production on Arctic shelves in
23
24 353 winter, driven by ice freezing and salt ejection is not likely to cease in a warmer climate, but rather
25
26 354 the opposite (Bitz et al. 2008, Ivanov and Watanabe 2013). There is also observational evidence that
27
28
29 355 cascading in the seasonally ice covered seas (e.g. the Barents Sea) is much more efficient than it is
30
31 356 in the permanently ice covered Arctic Ocean (Ivanov and Shapiro 2005). This gives us some
32
33 357 confidence that presented results are reasonable and have to be taken into account in future climate
34
35
36 358 scenarios. However, we acknowledge that such predictions should be considered with caution,
37
38 359 because of several uncertainties, which are caused by not taking into account in this study probable
39
40
41 360 additional 'actors'. First of all, the obtained results might be affected by the changing fresh water
42
43 361 content in the surface layer, which is likely going to increase due to excess summer melting.

44
45 362 Whether this extra fresh water stays in the area, where ice melted, or will be moved by surface
46
47
48 363 currents to the other region of the Arctic Ocean, or even, out of the Arctic Ocean (Mauritzen 2012),
49
50 364 is an open question? Recent observation-based studies (Morrison et al. 2012) suggest that, so far,
51
52 365 the excess melting and river runoff has led to substantial increase of fresh water content in the
53
54
55 366 Canadian Arctic, while in the Atlantic sector the opposite trend is true and a moderate salinity
56
57 367 increase is observed (MacPhee et al. 2009). As was pointed out in the introduction, the necessary
58
59 368 condition for effective dense water formation on shelf is the high frequency occurrence of strong
60
369 winds in a certain direction, which is able to break ice and open polynyas. Whether the wind pattern
370 is going to substantially change in the warmer climate is uncertain. We may only speculate that

1
2
3 371 under the given wind forcing the thinner ice, which is expected to dominate in the warmer climate,
4
5 372 could be easily broken and moved. As for the two analysed years, the SLP fields in the
6
7 373 corresponding winter months, reconstructed from the NCEP-NCAR reanalysis products
8
9
10 374 (<http://www.esrl.noaa.gov/psd/data/gridded/data.ncep.reanalysis.htm>), do not substantially differ.
11

12 375 In the beginning of this paper we also mentioned wind upwelling as the possible important
13
14 376 contributor to the shelf basin exchange in summer season under the depleted ice cover. We
15
16
17 377 compared the results of model calculation in summer months of 1987 and 2007 with respect to
18
19 378 possible upwelling intensification. However, no significant changes were found. This does not
20
21
22 379 mean that the concept of intensified upwelling in the warmer climate is compromised by this study.
23
24 380 We rather conclude that the reason behind this is the overestimation by the model of the summer ice
25
26 381 coverage in the Laptev Sea in 2007 (see Figure 4- c, f).
27
28
29 382

30
31 383 *Acknowledgements.* Authors would like to express their deep respect to Professor John Huthnance,
32
33 384 M.B.E. of the National Oceanographic Centre, whose fundamental contribution to the theory of
34
35
36 385 dense water cascading in the World Ocean inspired this investigation. We would like to thank our
37
38 386 former colleague Beverly de Cuevas from the National Oceanography Centre (NOC) for performing
39
40
41 387 model experiments. In AARI this study was supported by RFBR grant 13-05-41443 “Extreme
42
43 388 atmospheric events in the polar regions and its connection to changes in ice conditions”. At the
44
45 389 NOC this study was supported by the UK Natural Environment Research Council through the
46
47
48 390 Marine Centres' Strategic Research Programmes and is a contribution to the Arctic Research
49
50 391 Programme TEA-COSI project (Project ID: NE/I028947/1). The NOCS-ORCA simulations were
51
52 392 undertaken as part of the DRAKKAR collaboration (Barnier et al. 2006). NOC also acknowledges
53
54
55 393 the use of UK National High Performance Computing Resource. V. Ivanov is grateful to IARC
56
57 394 director Larry Hinzman for the given opportunity to finalize this paper during his two-month visit in
58
59 395 Fairbanks.
60

396

397

References

URL: <http://mc.manuscriptcentral.com/ggaf> Email: A.M.Soward@exeter.ac.uk

- 1
2
3 398 Aagaard, K., L.K. Coachman and E. Carmack. On the halocline of the Arctic Ocean. *Deep Sea Res.*
4
5 399 1981. 28A. 529-545.
6
7 400 Aksenov, Y., V. Ivanov, G. Nurser, S. Bacon, I. Polyakov, A. Coward, A. Naveira-Garabato, and A.
8
9
10 401 Beszczynska-Möller. The Arctic Circumpolar Boundary Current, *J. Geophys. Res.*, 2011. 116.
11
12 402 C09017, doi:10.1029/2010JC006637.
13
14 403 Bareiss, J. and K. Goergen. Spatial and temporal variability of sea ice in the Laptev Sea: Analysis
15
16 and review of satellite passiv-microwave data and model results, 1997 to 2002. *Global and*
17 404
18 *Planetary Change.* 2005. 48. 28–54.
19 405
20
21 406 Barnier, B., G. Madec, T. Penduff, J. M. Molines, A. M. Treguier, J. Le Sommer, A. Beckmann, A.
22
23 Biastoch, C. Böning, J. Dengg, C. Derval, E. Durand, S. Gulev, E. Remy, C. Talandier, S.
24 407
25 Theetten, M. Maltrud, J. McClean, and B. A. de Cuevas., Impact of partial steps and
26 408
27 momentum advection schemes in a global ocean circulation model at eddy permitting
28 409
29 resolution. *Ocean Dyn.* 2006. 56, 543-567. doi: 10.1007/s10236-006-0082-1.
30
31 410
32
33 411 Bitz, C.M., P.R. Gent, R. A. Woodgate, M. M. Holland and R. Lindsay. The influence of sea ice on
34
35 ocean heat uptake in response to increasing CO₂. 2008. *Journ. of Climate.* 19. 2437-2450.
36 412
37
38 413 Carmack, E. and D.C. Chapman). Wind-driven shelf/basin exchange on an Arctic shelf: The joint
39
40 roles of ice cover extent and shelf-break bathymetry. *Geophys. Res. Lett.* 30. 14. 1778.
41 414
42 doi:10.1029/2003GL017526.
43 415
44
45 416 Cavaliere, D., C. Parkinson, P. Gloersen and H. J. Zwally. Sea Ice Concentrations from Nimbus-7
46
47 SMMR and DMSP SSM/I-SSMIS Passive Microwave Data, 1979-2010. 1996, updated
48 417
49 yearly. Boulder, Colorado USA: National Snow and Ice Data Center. Digital media.
50 418
51
52 419 Dethleff, D. Linear model estimates of potential salt rejection and theoretical salinity increase in a
53
54 standardized water column of recurrent Arctic flaw leads and polynyas. *Cold Reg. Sci. and*
55 420
56 *Technol.* 2010. 61. 82–89.
57 421
58
59 422 Dmitrenko, I. A., S. A. Kirillov, L. B. Tremblay, D. Bauch, J. A. Hölemann, T. Krumpfen, H.
60
423 Kassens, C. Wegner, G. Heinemann and David Schröder. Impact of the Arctic Ocean

- 1
2
3 424 Atlantic water layer on Siberian shelf hydrography. *Journ. Geophys. Res.* 2010a. 115.
4
5 425 C08010. doi:10.1029/2009JC006020.
6
7 426 Dmitrenko, I. A., S. A. Kirillov, T. Krumpen, H., M. Makhotin, E. P. Abrahamsen, S. Willmes, E.
8
9
10 427 Bloshkina, H. Kassens, C. Wegner. Wind-driven diversion of summer river runoff
11
12 428 preconditions the Laptev Sea coastal polynya hydrography: Evidence from summer-to-
13
14 429 winter hydrographic records of 2007–2009. *Cont. Shelf Res.* 2010b. 30. 1656–1664.
15
16
17 430 Dmitrenko, I., S. Kirillov, V. Ivanov, R. Woodgate, I. Polyakov, N. Koldunov, L. Fortier, C.
18
19 431 Lalande, L. Kaleschke, D. Bauch, J. Hölemann, and L. Timokhov. Seasonal modification
20
21 432 of the Arctic Ocean intermediate water layer off the eastern Laptev Sea continental shelf
22
23 433 break. *Journ. of Geophys. Res.* 2009. 114. C06010. doi:10.1029/2008JC005229.
24
25
26 434 Encyclopaedia Britannica. Encyclopaedia Britannica Online Academic Edition. Encyclopædia
27
28 435 Britannica Inc. 2014. Available online at:
29
30
31 436 www.britannica.com/EBchecked/topic/637132/water-mass (Accessed . March 17 2014).
32
33 437 Environmental Working Group (EWG): Joint U.S.-Russian Atlas of the Arctic Ocean (CD-ROM).
34
35 438 1997, 1998. National Snow and Ice Data Centre, Boulder, Co. USA.
36
37
38 439 Fichfet, T., and M. A. M. Maqueda. Sensitivity of a global sea ice model to the treatment of ice
39
40 440 thermodynamics and dynamics, *Journ. of Geophys. Res.-Oceans.* 1997. 102. 12609-12646.
41
42
43 441 Frolov S.V., V.E. Fedyakov, V.Yu Tretyakov, A.E. Klain and G.V. Alexeev. New data on ice
44
45 442 thickness changes in the Arctic basin. *Doklady Earth Sciences (Doklady Akademii Nauk).*
46
47 443 2009. 425 (1). 104–108.
48
49
50 444 IPCC Forth Assessment Report: Climate Change 2007 (AR4). Available online at:
51
52 445 www.ipcc.ch/publications_and_data/publications_and_data_reports.htm (Accessed: March
53
54 446 17 2014).
55
56
57 447 Ivanov, V.V., G.I. Shapiro, J.M. Huthnance, D.L. Aleynik and P.N. Golovin. Dense water cascades
58
59 448 around the World Ocean. *Progr. Oceanogr.* 2004. 60. 47-98.
60
449 Ivanov V.V. and G.I. Shapiro. Formation of dense water cascade in the marginal ice zone in the
450 Barents Sea. *Deep Sea Res.* 2005. Part I. 52. 1699-1717.

- 1
2
3 451 Ivanov, V.V. and P.N. Golovin. Observations and modeling of dense water cascading from the
4
5 452 Laptev Sea shelf. *Journ. of Geophys. Res.* 2007. 112. C09003. doi:10.1029/2006JC003882.
6
7 453 Ivanov, V.V., I.V. Polyakov, I.A. Dmitrenko, E. Hansen, I.A. Repina, S.S. Kirillov, C. Mauritzen,
8
9
10 454 H. Simmons, L.A. Timokhov. Seasonal Variability in Atlantic Water off Spitsbergen. *Deep*
11
12 455 *Sea Res. Part I.* 2009. 56. 1-14. doi:10.1016/j.dsr.2008.07.013.
13
14 456 Ivanov V.V. and E. Watanabe. Does Arctic sea ice reduction foster shelf–basin exchange?
15
16
17 457 *Ecological Applications*, 2013. 23(8). 1765–1777.
18
19 458 Ivanov, V.V. and Ye. Aksenov. Atlantic Water transformation in the eastern Nansen Basin:
20
21 459 observations and modelling, *Probleme Arctiki i Antarktiki*. 2013. 1 (95). 72-86 (in Russian
22
23
24 460 with English abstract).
25
26 461 Jackson, J.M., C. Lique. M. Alkire, M. Steele. C.M. Lee, W.M. Smethie and P. Schlosser. On the
27
28
29 462 waters upstream of Nares Strait, Arctic Ocean, from 1991 to 2012. *Cont. Shelf Res.* 73. 83-
30
31 463 96. ISSN 0278-4343. Available online at: <http://dx.doi.org/10.1016/j.csr.2013.11.025>
32
33 464 (Accessed: March 17 2014).
34
35
36 465 Jahn, A., Ye. Aksenov, B.A. de Cuevas, L. de Steur, S. Häkkinen, E. Hansen, C. Herbaut, M.-N.
37
38 466 Houssais, M. Karcher, F. Kauker, C. Lique, A. Nguyen, P. Pemberton, D. Worthen, and J.
39
40 467 Zhang. Arctic Ocean freshwater: How robust are model simulations? *Journ. Geophys. Res.*
41
42
43 468 2012. 117. C00D16. doi:10.1029/2012JC007907.
44
45 469 Johnson, M., A. Proshutinsky, Ye. Aksenov, A. YT. Nguyen, R. Lindsay, C. Haas, J. Zhang, N.
46
47
48 470 Diansky, R. Kwok, W. Maslowski, S. Hakkinen, I. Ashik, and B. de Cuevas. Evaluation of
49
50 471 Arctic sea ice thickness simulated by Arctic Ocean Model Intercomparison Project models.
51
52 472 *Journ. of Geophys. Res.* 2012. 117. C00D13. doi:10.1029/2011JC007257
53
54
55 473 Kampf, J. (2005). Cascading-driven upwelling in submarine canyons in high latitudes. *J. Geophys.*
56
57 474 *Res.*, 110, C02007, doi:10.1029/2004JC002554.
58
59
60

1

2

3

4

5

6

7

8

9

10

11

12

13

14

15

16

17

18

19

20

21

22

23

24

25

26

27

28

29

30

31

32

33

34

35

36

37

38

39

40

41

42

43

44

45

46

47

48

49

50

51

52

53

54

55

56

57

58

59

60

475 Karcher, M., Smith, J. N., Kauker, F., Gerdes, R., and Smethie, W. M.. Recent changes in Arctic
476 Ocean circulation revealed by iodine- 129 observations and modeling. *J. Geophys. Res.*
477 117(C8). 2012.

479 Krumpen, T., M. Janout, K. I. Hodges, R. Gerdes, F. Girard-Arduin, J. A. Holemann and S.
480 Willmes. Variability and trends in Laptev Sea ice outflow between 1992 – 2011. Available
481 online at: [www.the-cryosphere-discuss.net/6/C2777/2013/tcd-6-C2777-2013-](http://www.the-cryosphere-discuss.net/6/C2777/2013/tcd-6-C2777-2013-supplement.pdf)
482 [supplement.pdf](http://www.the-cryosphere-discuss.net/6/C2777/2013/tcd-6-C2777-2013-supplement.pdf) (Accessed: March 17 2014).

483 Kwok, R., C.F. Cunningham, M. Wesnahan, I. Rigor, H.J. Zwally, and D. Yi. (2009). Thinning and
484 volume loss of the Arctic Ocean ice cover: 2003-2008, *J. Geophys. Res.* 114, C07005,
485 doi:10.029/2009JC005312.

486 Lique, C. A. M. Treguier, M. Scheinert, and T. Penduff. A model-based study of ice and freshwater
487 transport variability along both sides of Greenland. *Clim. Dyn.* 2009. 33. 685-705,
488 doi:10.1007/s00382-008-0510-7.

489 Lique, C. and M. Steele. Where can we find a seasonal cycle of the Atlantic water temperature
490 within the Arctic Basin? *Journ. Geophys. Res.* 2012. 117. C03026.
491 doi:10.1029/2011JC007612.

492 Madec, G., M. Delecluse, M. Imbard, and C. Levy. OPA version 8.1 ocean general circulation
493 model reference manual. Tech. Rep. 1998. 91 pp. Available online at: [www.nemo-](http://www.nemo-ocean.eu)
494 [ocean.eu](http://www.nemo-ocean.eu) (Accessed: March 17 2014).

495 Maqueda, M.A., A.J. Willmott and N.R.T. Biggs. Polynya dynamics: a review of observations and
496 modelling. *Rev. Geophys.* 2004. 42. RG1004.

497 Martin, S., Cavalieri, D.J. Contributions of the Siberian shelf polynyas to the Arctic Ocean
498 intermediate and deep water. *Journ. of Geophys. Res.* 94. C9, 12725- 12738.

499 Mauritzen, C. Arctic freshwater. *Nature Geoscience.* 2012. 5. 162-164.

1

2

3

4

5

6

7

8

9

10

11

12

13

14

15

16

17

18

19

20

21

22

23

24

25

26

27

28

29

30

31

32

33

34

35

36

37

38

39

40

41

42

43

44

45

46

47

48

49

50

51

52

53

54

55

56

57

58

59

60

500 McPhee, M.G., A. Proshutinsky, J. H. Morison, M. Steele and M. B. Alkire. Rapid change in
501 freshwater content of the Arctic Ocean. *Geophys. Res. Lett.* 2009. 36. L10602
502 doi:10.1029/2009GL037525.

503 Morrison, J., R. Kwok, C. Peralta-Ferris, M. Alkire, I. Rigor and M. Steele. Changing Arctic
504 Ocean freshwater pathways. *Nature*. 2012. 481. 66-70. doi:10.1038/nature10705.

505 Nikiforov, Ye. G., and A. O. Shpaikher, Features of the formation of hydrological regime large-
506 scale variations in the Arctic Ocean. 1980. (Gydrometeoizdat, Leningrad) (in Russian).

507 Pease, C.H. The size of wind-driven coastal polynyas. *Journ. of Geophys. Res.* 1987. 92. C7. 7049-
508 7059.

509 Pickart, R.S., G.W.K. Moore, D.J. Torres, P.S. Fratantoni, R.A. Goldsmith, and J. Yang. Upwelling
510 on the continental slope of the Alaskan Beaufort Sea: Storms, ice, and oceanographic
511 response. *Journ. of Geophys. Res.* 2009. 114, C00A13. Available online at:
512 www.dx.doi.org/10.1029/2008JC005009 (Accessed: March 17 2014).

513 Polyakov I., A. Beszczynska, E.C. Carmack, I.A. Dmitrenko, E. Fahrbach, I.E. Frolov, R. Gerdes,
514 E. Hansen, J. Holfort, V.V. Ivanov, M.A. Johnson, M. Karcher, F. Kauker, J. Morison,
515 K.A. Orvik, U. Schauer, H.L. Simmons, Ø. Skagseth, V.T. Sokolov, M. Steele, L.A.
516 Timokhov, D. Walsh and J.E. Walsh J.E. One more step towards a warmer Arctic.
517 *Geophys. Res. Lett.* 2005. 32. L17605. 1-4. doi: 10.1029/2005GL023740.

518 Proshutinsky A.Y. and Johnson M.A. Two circulation regimes of the wind driven Arctic Ocean.
519 *Journ. Geophys. Res.* 1997. 102. 12493-12514.

520 Proshutinsky, A., Ye. Aksenov, J. Clement-Kinney, R. Gerdes, E. Golubeva, D. Holland, G.
521 Holloway, A. Jahn, M. Johnson, E. Popova, M. Steele, and E. Watanabe. Recent advances
522 in Arctic Ocean studies employing models from the Arctic Ocean Model Intercomparison
523 Project. *Oceanography*. 2011. 24. 102-113.

524 Rainville, L., C.M. Lee, and R.A. Woodgate. Impact of wind-driven mixing in the Arctic Ocean.
525 *Oceanography*. 2011. 24(3).136–145. Available online at:
526 www.dx.doi.org/10.5670/oceanog.2011.65 (Accessed: March 17 2014).

1

2

3

4

5

6

7

8

9

10

11

12

13

14

15

16

17

18

19

20

21

22

23

24

25

26

27

28

29

30

31

32

33

34

35

36

37

38

39

40

41

42

43

44

45

46

47

48

49

50

51

52

53

54

55

56

57

58

59

60

527 Rudels, B., E.P. Jones, L.G. Anderson, and G. Kattner. On the intermediate depth waters in the
528 Arctic Ocean. In: *The Polar Oceans and their Role in Shaping the Global Environment*,
529 AGU Geophys. Monograph 85, edited by O.M Johannessen, R.D. Muench, and J.E.
Overland, pp. 33-46, 1994 (Washington D.C.)

531 Rudels, B., R.D. Muench, J. Gunn, U. Schauer and H.J. Friedrich. Evolution of the Arctic Ocean
532 boundary current north of the Siberian shelves. *Journ. Marine Syst.* 2000. 25. 77-99.

533 Rudels, B. Arctic Ocean circulation and variability – advection and external forcing encounter
534 constraints and local processes. *Ocean Science.* 2012. 8. 261–286.

535 Shapiro, G.I., J.M. Huthnance, V.V. Ivanov. Dense water cascading off the continental shelf *Journ.*
536 *of Geophys. Res.* 2003. 108. C12. art: no 3390.

537 Stroeve, J. C., M.C. Serreze, M.M. Holland, J.E. Kay, J. Malanik, A.P. Barrett. The arctic's rapidly
538 shrinking sea ice cover: a research synthesis. *Clim. Change.* 2011. 110 (3). 1005-1027.
539 Available online at: www.dx.doi.org/10.1007/s10584-011-0101-1 (Accessed: March 17
540 2014).

541 Wiese, W., 1948, *Morya Sovetskoy Arktiki*, 1948. (Moscow-Leningrad) (in Russian).

Figure captions

544 Figure 1. The study area. Smoothed bottom topography of the shelf-slope is shown by solid lines.
545 Polygon marks the region, where flux calculations were performed.

546 Figure 2. Time series of ice extent (15% concentration) according to satellite data: open circles
547 denote winter season (Dec – May), triangles denote summer season (Jun – Nov) (Cavalieri
548 1996, <http://nsidc.org/data/nsidc-0051.html>).

549 Figure 3. Mean monthly ice concentration in 1986-87: September-1986, April-1987, September-
550 1987 according to satellite data (a, b, c) and model (d, e, f) respectively.

551 Figure 4. Mean monthly ice concentration in 2006-07: September-2006, April-2007, September-
552 2007 according to satellite data (a, b, c) and model calculations (d, e, f) respectively.

553 Figure 5. Model distribution of monthly mean temperature, °C, and current speed, cm/s at 250 m

1
2
3
4
5
6
7
8
9
10
11
12
13
14
15
16
17
18
19
20
21
22
23
24
25
26
27
28
29
30
31
32
33
34
35
36
37
38
39
40
41
42
43
44
45
46
47
48
49
50
51
52
53
54
55
56
57
58
59
60

554 depth in September, 1986 (a) and 2007 (b).

555 Figure 6. Model temperature distribution ($^{\circ}\text{C}$) at 250 m throughout 2006-07: (a) Sep-2006; (b) Feb-
556 2007; (c) Mar-2007; (d) Apr-2007; (e) May-2007; (f) Jul-2007; (g) Aug-2007; (h) Sep-
557 2007. Contours show smoothed temperature field.

558 Figure 7. Time series of maximum and minimum temperature at 250 m depth in 1986-87 and 2006-
559 07: Tmax in 1986-87 - open squares; Tmax in 2006-07 - open circles; Tmin in 1986-87 -
560 crosses; Tmin in 2006-07 - triangles.

561 Figure 8. Temperature ($^{\circ}\text{C}$) and salinity (PSU) distribution at the vertical section along 80°N in
562 April 1987 (a,c) and in April 2007 (b,d) respectively.

563 Figure 9. Vertical distribution of mean cross-slope speed of flow, m/s (a, d); specific heat flux,
564 W/m^2 (b, e); salt flux, g/m^2 (c, f) in March - May 1987 and 2007. Spatial averaging is
565 done over depth contours with lateral bounds, shown in Figure 1.

The differences in the pan-Arctic circulation between September 1987 and 2007

Figure S1 shows the change in the modelled September ocean upper circulation and water temperature at 250 m depth between 1987 and 2007. The depth corresponds to the upper part of the Atlantic water residing in the Arctic Ocean. The principal difference is that in 1987 Atlantic Water extended farther in the central Arctic Ocean than in 2007, bringing anomalously warm waters in the Amundsen Basin and in the Makarov Basin. According to the model, the upper intermediate ocean circulation in the Arctic Ocean in September 1987 was cyclonic (counter-clockwise), with the Arctic boundary current along the Siberian shelf slope being strong and narrow, consistent with the other high-resolution modelling studies (e.g. Aksenov et al 2011). In the present simulations the boundary current extended all way to the Canada Basin, where the upper part of the current became unstable in the vicinity of the Chukchi Plateau, but still followed cyclonically the Alaskan coast and then the northern shelf slope of the Canadian Arctic Archipelago, finally forming a strong shelf slope jet flowing towards Fram Strait (Figure S1-a). In contrast, in September 2007 most of the warm Atlantic inflow followed the shelf slopes of the Barents and Kara Seas and the temperature of the inflow was higher than in 1987 (Figure S1-a,b). The cyclonic boundary flow along the western Siberian shelf slope was also strong but wider. Two jets branched from the current into the Arctic Ocean interior, one along the Lomonosov Ridge and another along the Mendeleev Ridge with the Arctic boundary current being essentially blocked in the Canada Basin. Instead, the circulation in the Canada Basin from the surface down to ca. 300 m was anti-cyclonic (clockwise), coinciding with the circulation in the Beaufort Gyre (Figure S1-b). The blocking effect was also simulated in the other models, for more discussion please see e.g., Karcher et al. (2012). Whereas the changes which occurred between 1987 and 2007 in the Arctic boundary current along the shelf slopes of the Kara, Laptev and East-Siberian Seas were due to the combined effects of the intensified shelf-basin exchanges and the variations in the Atlantic water inflow, we attribute the difference in the ocean circulation in the Canada Basin between these two years to the difference in the large-scale wind field in the Arctic, with anti-cyclonic winds in 2007 dominating over the Canada Basin (e.g.

1
2 27 McPhee et al. 2009; Proshutinsky et al. 2011). More analysis, which is beyond the scope of the
3
4 28 present study, is needed to differentiate between local and large-scale causes of the changes in the
5
6 29 Arctic Ocean circulation.
7
8

9 30

11 31 **Formation of dense water on the north-western shelf of the Laptev Sea**

12
13
14 32 Mapping of anomaly propagation near the seabed is very helpful when describing
15
16 33 cascading events (e.g. Ivanov and Golovin 2007). A brief description of the evolution of
17
18 34 thermohaline structure near the seabed on the north-western Laptev Sea shelf is given below and
19
20
21 35 illustrated by Figure S2.
22

23 36 In the fall-early winter 2006 thermohaline convection reaches seabed over shallow banks
24
25 37 (about 50 m depth) between 79 °N and 81°N. Throughout November and December temperature
26
27 38 drops to the freezing point (Figure S2- j, k) and salinity over the shelf decreases (Figure S2- a,b)
28
29 39 because of thermal convection, which mixes up fresher surface water with saltier deep water. In
30
31 40 January and February 2007, the spot of near to freezing temperature over the shelf increases in size
32
33 41 (Figure S2- l ,m), while salinity is increasing, because of haline convection, induced by ice
34
35 42 formation (Figure S2- c, d). From March to May salinity on the shelf is steadily increasing, due to
36
37 43 recurrent polynya opening and intensive ice formation. The size of the high salinity area grows and
38
39 44 expands offshore and downslope (Figure S2- e, f, g). Downslope and offshore propagation of the
40
41 45 dense water plume and its mixing with the surrounding water is also visualized by the drop in
42
43 46 temperature of Atlantic water (AW): From November to March, the location of the AW layer is
44
45 47 indicated by a positive temperature stripe (Figure S2- i - m), stretched along the continental margin.
46
47 48 Starting from April, the continuity of AW layer is interrupted in the region where dense water
48
49 49 intrusions from shelf occur (79 - 82°N). The cold segment, sitting in the AW warm pool, moves
50
51 50 south-east, indicating the propagation of the intrusion-affected AW portion along the continental
52
53 51 margin. The June plots of salinity and temperature (Figure S2- h, p) show the final stage of the
54
55 52 process: the high salinity area on the shelf merges with the zone of similar salinity in the deep
56
57
58
59
60

1
2 53 water, forming a wide band of high salinity water over shelf and slope. The main dense water pool
3
4 54 is incorporated in the AW flow. Its location in June is roughly between 77°30'N and 79°N (Figure
5
6
7 55 S2- p). It is indicated by low temperature (about 0°C), but could not be identified by salinity, which
8
9 56 is about the same is in the core of AW layer at this position. It is also important to note that the
10
11 57 thermohaline structure on the shallow shelf to the south of 77°30'N has not radically changed
12
13
14 58 throughout the winter of 2006-2007. Extremely low salinity in this area, caused by intensive river
15
16 59 water inflow, prevents formation of sufficiently dense water to cascade down the continental slope
17
18 60 (Ivanov et al. 2004).
19
20
21 61

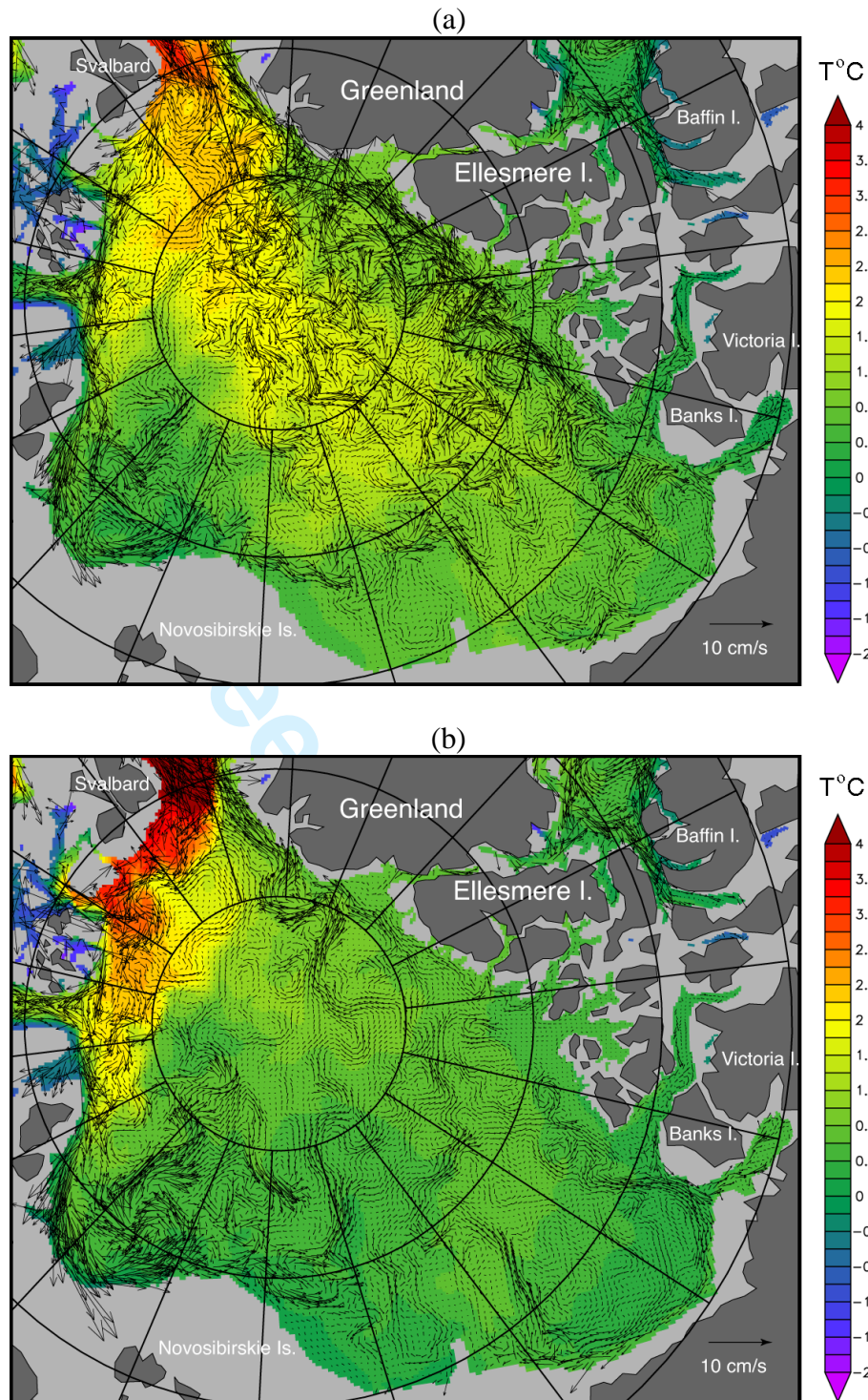
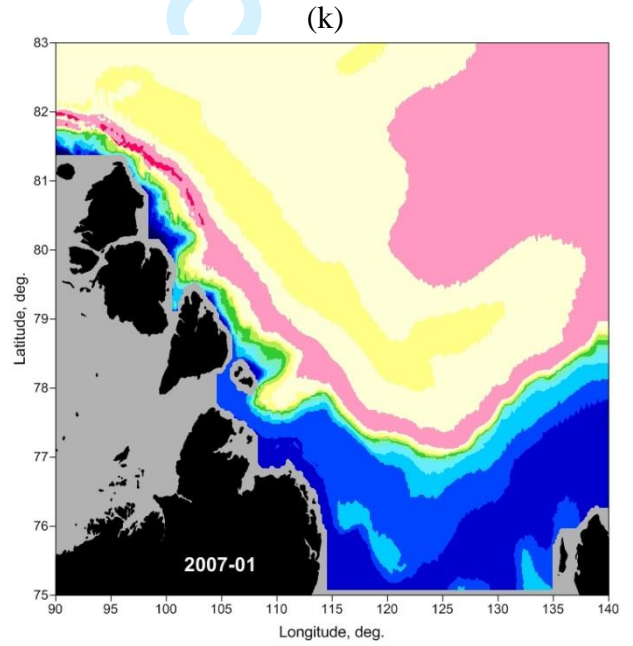
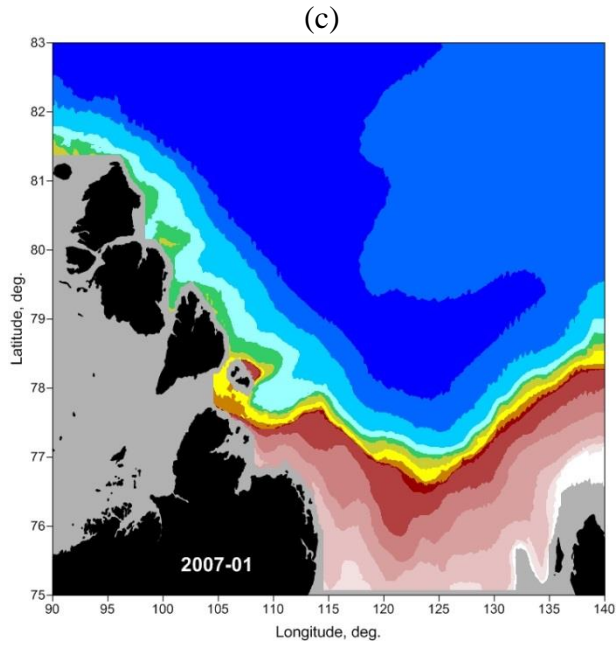
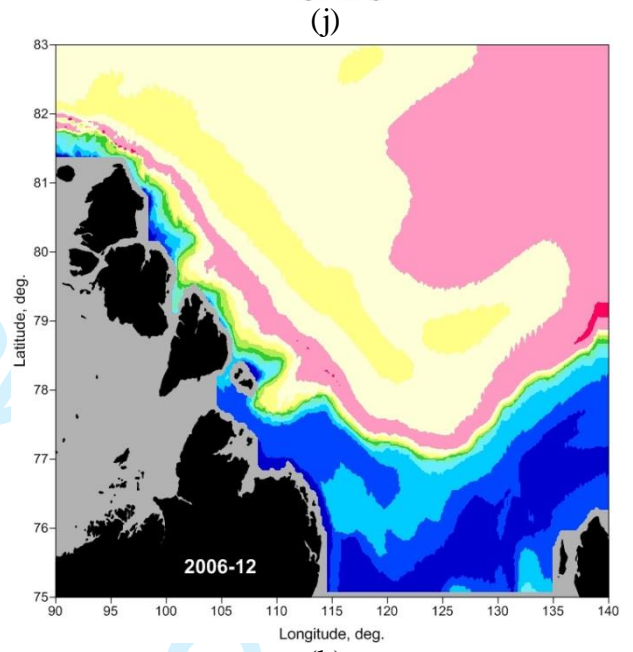
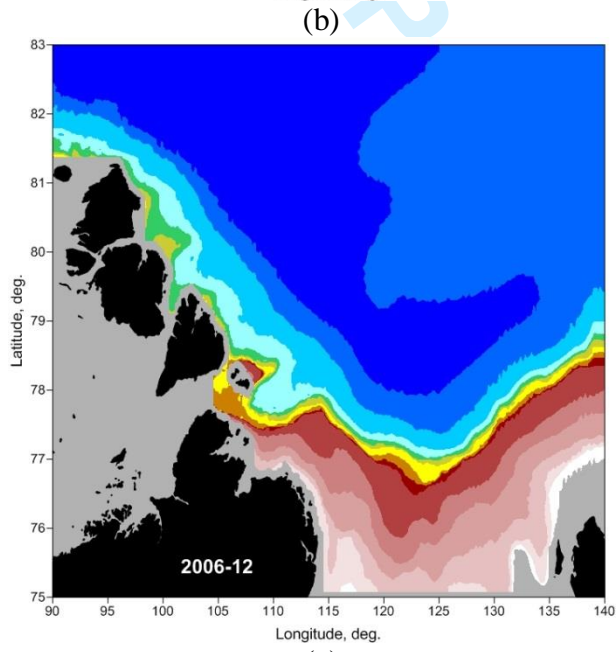
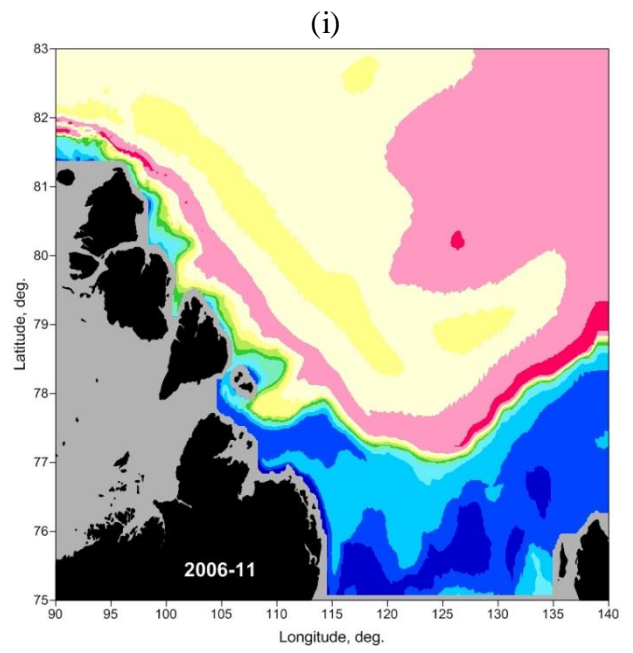
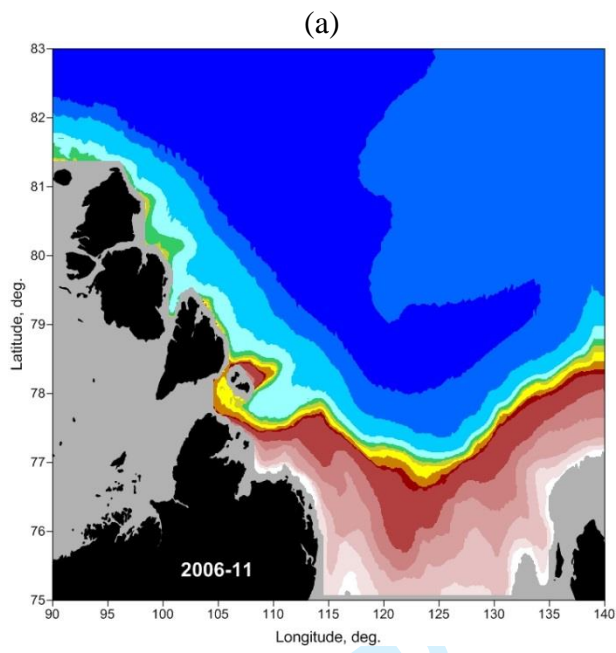
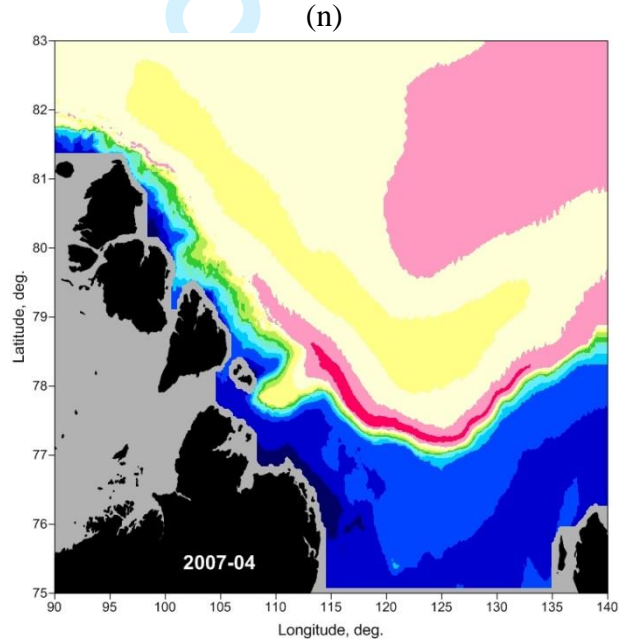
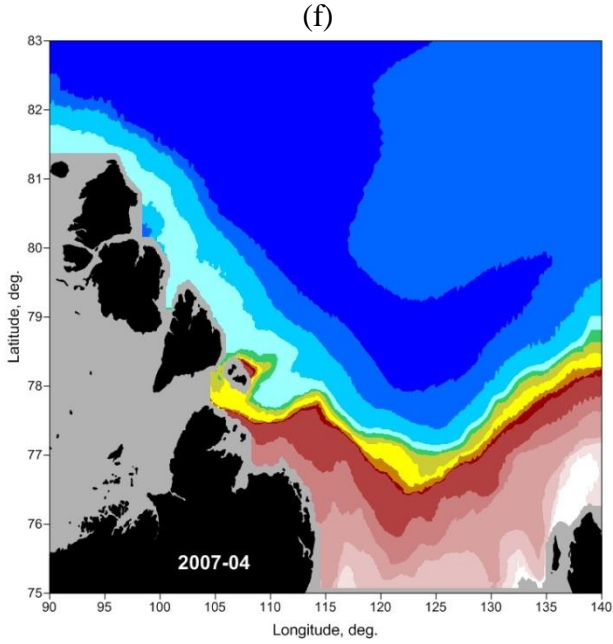
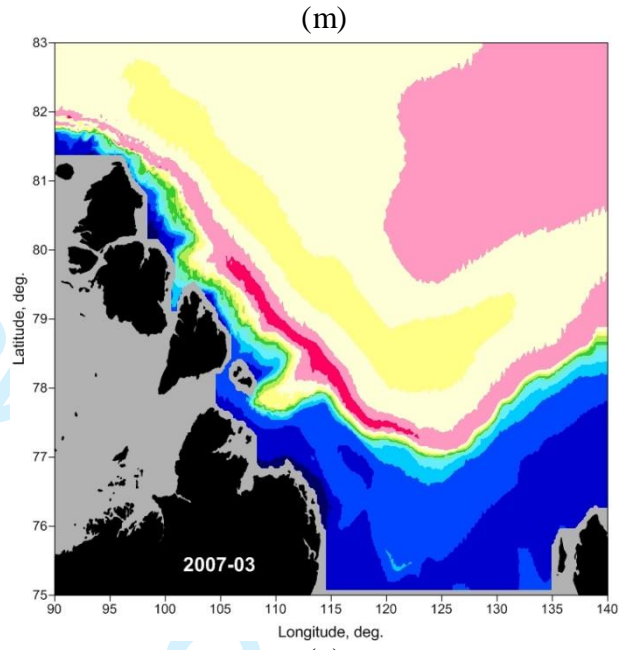
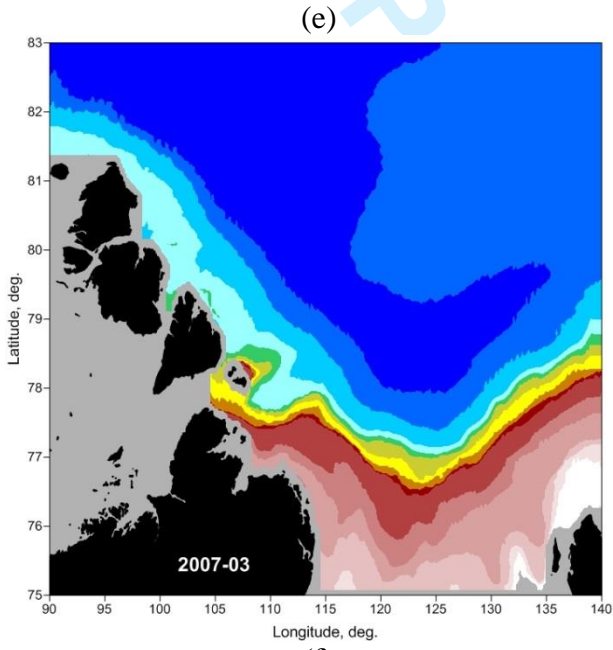
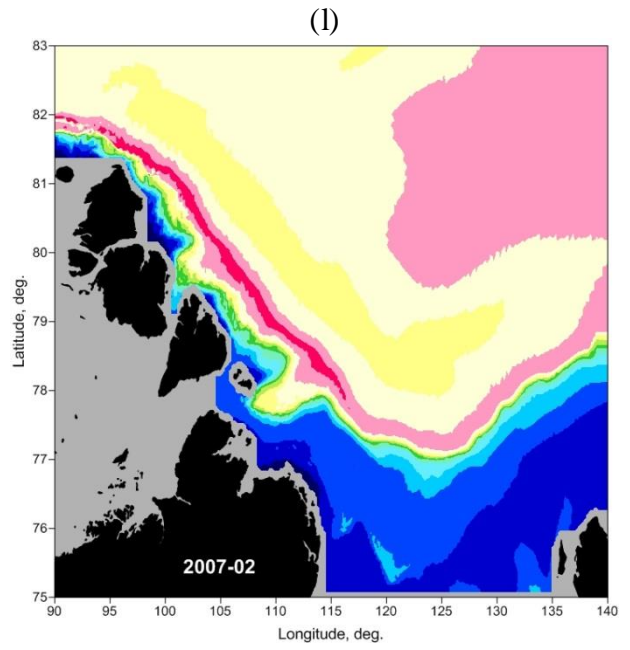
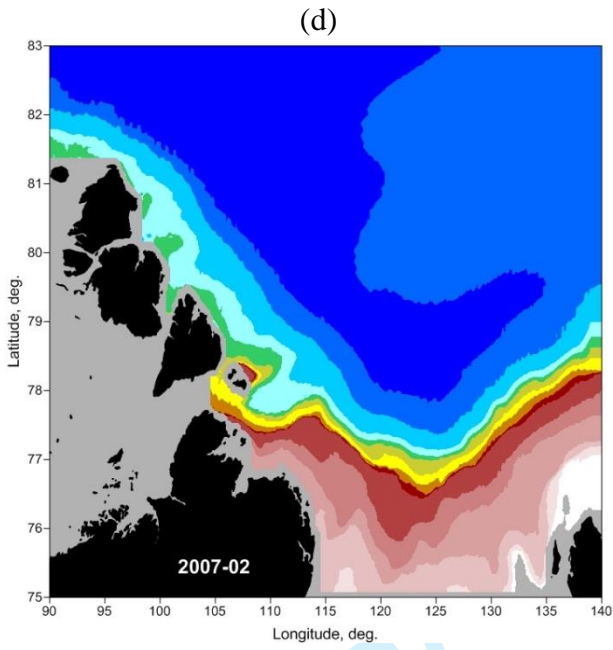


Figure S1. September monthly temperature (colour) and ocean velocity (vectors) at the 250 m depth in 1987 (a) and 2007 (b). The velocity scale is shown in the insert. Results from the NOCS-ORCA simulations.



1
2
3
4
5
6
7
8
9
10
11
12
13
14
15
16
17
18
19
20
21
22
23
24
25
26
27
28
29
30
31
32
33
34
35
36
37
38
39
40
41
42
43
44
45
46
47
48
49
50
51
52
53
54
55
56
57
58
59
60



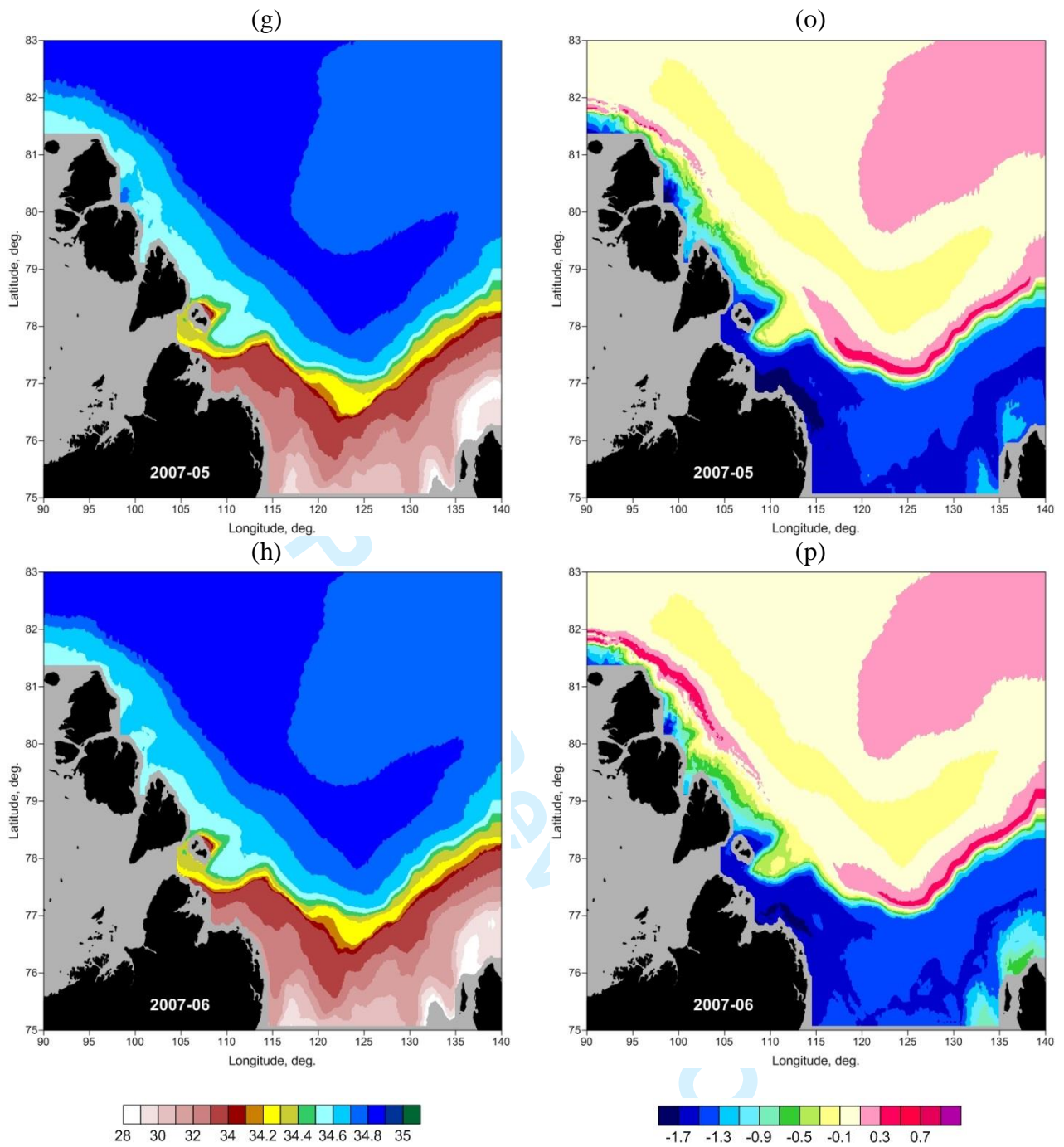


Figure S2. Evolution of average monthly salinity (a – h) and temperature (i – p) near the seabed (s-level 2) throughout the winter 2006-2007.

65